sustainability

MDPI

Article

Multi-Scenario Simulation of Construction Land-Use Change and Ecosystem Service Value Response for Resilient and Sustainable Built Environment Optimization: A Case Study of Xi'an, China

Yingqi Lin [1], Shutao Zhou [1], Chulun Sun [2] and Weina Zhou [1,*]

[1] Department of Architecture and Environmental Art, Xi'an Academy of Fine Arts, Xi'an 710065, China; linyingqi2001@163.com (Y.L.); m19591281210@163.com (S.Z.)
[2] Academy of Arts & Design, Tsinghua University, Beijing 100084, China; 13021103572@163.com
* Correspondence: 19906960980@163.com; Tel.: +86-199-0696-0980

Abstract

With the Qinling ecological barrier located in the south, the Guanzhong Plain's agricultural systems in the central–north, and urban construction expanding outward, Xi'an represents a typical western Chinese metropolis where multiple land functions compete within a limited territory. Such spatial overlap exerts considerable stress upon the provisioning of regional ecosystem services. To ascertain how different land-use configuration trajectories might affect ecological outcomes, this study couples multi-objective programming (MOP), a PLUS-based spatial allocation model, ecosystem service value (ESV) accounting, a sensitivity index (SI), and a local response index (LRI). Historical land-use cartographic datasets for 2000, 2010, and 2020 were mobilized to identify transitions, validate the simulation framework, and generate prospective land-use configuration projections for 2040 across four policy pathways: status quo continuation, growth-oriented, ecological–conservation-preferred, and balanced. The retrospective analysis reveals a clear north–south dichotomy: forests dominate the southern Qinling range, cropland occupies the central and northern plains, and built-up areas have progressively encroached into peripheral cropland, which serves as the primary source of new construction. For 2040, simulated ecological performance differs markedly across scenarios. The conservation-priority pathway yields the largest ESV, totaling 3.317×10^{10} CNY—6.64% higher than the 2020 baseline. In contrast, the growth-oriented pathway gives the smallest ESV, 2.948×10^{10} CNY, representing a 5.24% reduction. In 2020, forest land alone contributed 79.7% of the total ESV, remaining the dominant contributor. According to the SI and LRI outcomes, positive ESV shifts are mainly concentrated in the Qinling piedmont transitional zone, Lantian County, and southeastern Chang'an District, whereas negative shifts are tightly coupled with zones of urban expansion. Taken together, these results imply that future spatial planning in Xi'an should give top priority to safeguarding the Qinling ecological system, curbing construction land growth along the agricultural–urban interface, and promoting blue-green infrastructure renewal within already built-up areas.

Keywords: land use transition; ecosystem service value response; multi-scenario land use simulation; coupled MOP-PLUS framework; local response index (LRI); territorial spatial zoning

Check for updates

Academic Editor: Maria Rosa Trovato

Received: 9 May 2026
Revised: 14 June 2026
Accepted: 24 June 2026
Published: 30 June 2026

Copyright: © 2026 by the authors. Licensee MDPI, Basel, Switzerland. This article is an open access article distributed under the terms and conditions of the Creative Commons Attribution (CC BY) license.

1. Introduction

Within Xi'an, three concurrent processes define territorial development: construction land keeps expanding, agricultural space undergoes adjustment, and ecological land is subject to protection measures. Such land use transitions directly affect how regional ecosystems function and perform, particularly in terms of food provisioning, climate regulation, water retention, and biodiversity support [1,2]. Within fast-urbanizing regions, built-up area growth typically encroaches on cropland, shrinks ecological space, and raises the proportion of impervious surfaces. Consequently, carbon storage may decline, hydrological and climatic regulation may weaken, habitat maintenance may be disrupted, and risks like urban heat islands, flooding, and reduced ecological well-being may intensify [3,4]. Modifications to agricultural space also influence food supply, farmland preservation, and rural ecosystem stability. Meanwhile, the fragmentation within forest, grassland, and aquatic systems restricts the constraints on regional ecosystem service provision. Emerging evidence indicates that altering land use structures in urbanizing areas can modify both the magnitude and spatial pattern of ecosystem service values [5,6]. As China shifts from an expansion-driven growth model toward high-quality development, territorial spatial governance must reconcile urban expansion, cropland conservation, and ecological security [7,8]. Hence, assessing the responsiveness of ecosystem service values to values responding to alternative land-use trajectories is critical for guiding territorial spatial optimization and fostering regional sustainability.

The existing literature relevant to this work falls into three methodological categories: simulating land use change, optimizing land demand, and evaluating ecological impacts. Land use simulation. Early investigations often relied on Markov chains, system dynamics (SD), together with CA–Markov formulations, modeling approaches for forecasting land use quantities as well as conversion dynamics. Subsequently, spatially aware frameworks—including CLUE-S, FLUS, and PLUS—emerged, offering enhanced capabilities for allocating future land use patterns across space. Unlike conventional transition-driven approaches, PLUS integrates two distinctive features: land expansion analysis and a patch-generation mechanism. These enable the model to uncover the underlying determinants behind land-use proliferation and to simulate patch-wise spatial transformation and spatial evolution [6,9,10]. Land demand optimization. The multi-objective programming approach (MOP) provides an operational pathway for distributed land use areas subject to multiple constraints—such as economic growth, ecological conservation, farmland protection, and built-up land needs. When MOP is coupled with PLUS, the optimized land quantities derived from MOP can be converted into spatially explicit simulations, thus bridging the gap between quantity optimization and spatial allocation [11–14]. ESV-based ecosystem-service valuation assessment supplies a monetized metric for contrasting the ecological outcomes of alternative land use configurations. A growing number of recent studies have combined scenario simulation tools (e.g., MOP and PLUS) with ESV assessment to compare ecological performance across different development trajectories, thereby supporting spatial optimization and sustainable land governance [15–19].

Despite progress in multi-scenario land use simulation and ESV assessment, existing studies still face several shortcomings when it comes to connecting simulation outputs, response detection, and spatial policy measures. First, while some research has prospective land-use configurations, scenario-tailored land use patterns, and scenario-specific land demand, it is often specified either by extrapolating historical trends or by relying on empirical assumptions. Meanwhile, other work has attempted to optimize quantitative land use structures, but such efforts are seldom tightly linked to spatially explicit simulations. Consequently, it remains difficult to capture how both the areal composition and the locational configuration across land-use types evolve concomitantly under alternative

scenarios [19–22]. Second, a large portion of ESV-oriented investigations concentrate on changes in aggregate value or on the relative contributions of individual land use categories across different scenarios. Yet relatively little attention has been given to the precise locations where ESV gains or losses take place, the magnitude of those changes, or the spatial processes that drive them [23–27]. Third, although the overall sensitivity index can capture the regional-scale response of ESV to land use changes, it is not well suited for detecting where positive versus negative responses occur within local spatial units, nor for revealing their spatial heterogeneity [15,24,28,29]. Furthermore, how ecological protection, farmland preservation, and urban expansion interact with each other under the constraints imposed by territorial spatial planning—such as ecological redlines, permanent basic farmland boundaries, and urban growth limits—remains an issue that requires deeper investigation [30–33].

Xi'an offers an ideal context for investigating the interactions between land-use dynamics and ecosystem-service valuation (ESV), as three distinct yet interwoven territorial functions coexist within its administrative boundaries: the Qinling Ecological Barrier to the south, the agricultural landscapes of the Guanzhong Plain across the central and northern parts, and the continuously expanding built-up areas surrounding the metropolitan core. This spatial arrangement creates persistent trade-offs and tensions among ecological security, farmland preservation, and urban growth. Previous studies have demonstrated that land-use transformations documented in Xi'an during the preceding two decades are strongly associated with fluctuations in ESV. Moreover, issues such as protecting the Qinling Ecological Barrier, restoring ecosystems in the Weihe River Basin, and curbing urban sprawl have become central concerns in Xi'an's territorial spatial governance [25,34,35]. Against this backdrop, projecting future land–system trajectories alongside assessing the associated corresponding ecosystem service–value responses can help clarify how alternative development pathways may reshape land use composition, ecological consequences, and spatial trade-offs. Such analyses are valuable for supporting spatial optimization and coordinated ecological governance in fast-urbanizing regions [36–38]. Accordingly, this study proposes an integrated analytical framework—MOP-PLUS-ESV-SI/LRI—that links land use quantity optimization, spatial pattern simulation, ESV accounting, and response detection. In addition to predicting future land use patterns, the study also evaluates total ESV changes, local response characteristics, and variations at the administrative-unit scale across different scenarios. This framework is designed to reveal spatial trade-offs among three competing priorities: ecological protection in the Qinling Mountains, cropland conservation on the Guanzhong Plain, and urban construction expansion [39–42]. Specifically, this study seeks to answer the following three research inquiries:

(1) What were land-use transformations structured as well as spatial patterns within Xi'an between 2000 and 2020?
(2) How will land use patterns and ESV differ across the four development scenarios projected for 2040?
(3) How does the overall sensitivity, local response, and administrative-unit-scale heterogeneity of ESV vary with respect to relation to land-system change, as well as what implications do these variations hold for territorial spatial optimization?

2. Study Region and Data Inputs

2.1. Overview of the Study Area

The city of Xi'an, situated in Shaanxi Province (China), serves as the focal area for this investigation. Its geographical coordinates span from 33°42′ N to 34°45′ N and 107°40′ E to 109°49′ E, covering roughly 10,100 km^2. As a key metropolitan center in western China, Xi'an encompasses diverse land uses within a single administrative boundary—namely, a

central built-up core, surrounding new towns, productive agricultural plains, and the ecologically significant southern Qinling mountain belt. This particular configuration makes Xi'an a representative case for studying how urban sprawl, farmland conservation, and ecological protection interact with one another. As illustrated in Figure 1, Xi'an lies between the Qinling Ecological Barrier and the Guanzhong Plain. The southern Qinling range supplies the primary ecological services underpinning regional security, whereas the central and northern sections within the Guanzhong Plain support agricultural output, population agglomeration, and urban development. In terms of topography, the city slopes downward from the southern mountains toward the northern lowlands and tablelands. Specifically, the south is occupied by the Qinling Mountains, while the central sector consists mainly of the Weihe River alluvial plain, and the northern part features loess tablelands together with hilly transition zones. This topographic framework gives rise to a clearly differentiated land use pattern: forests dominate the southern Qinling belt, croplands are primarily found in the Weihe Plain and the northern loess tablelands, and impervious construction land concentrates in the central urban area along with its peripheral expansion zones. Xi'an was selected as the study site because its natural ecological assets, accelerated urbanization, and challenges of territorial spatial governance are deeply intertwined. The Qinling range acts as the region's ecological anchor, the Guanzhong Plain serves as the primary agricultural zone, and the central city plus its surrounding clusters form the main arena for construction land growth. Over the period 2000–2020, built-up areas progressively extended toward urban peripheries, transport corridors, and the central-northern plain, with cropland conversion becoming increasingly pronounced. This trend heightened conflicts among urban development, farmland protection, and ecological integrity. The outward growth of construction land has intruded into both agricultural and ecological spaces, thereby impairing cropland preservation and the delivery of ecosystem services across the Guanzhong Plain. Within high-density built zones, a lack of adequate blue-green space restricts climate regulation, hydrological control, and recreational services. Moreover, the piedmont transitional belt along the northern Qinling slope has experienced disturbance from urban construction, transport infrastructure projects, and tourism activities—pressures that may weaken ecological corridor connectivity and water retention capacity. Consequently, Xi'an represents an appropriate case for analyzing the interactions among the Qinling Ecological Barrier, the agricultural lands of the Guanzhong Plain, and ongoing urban construction expansion.

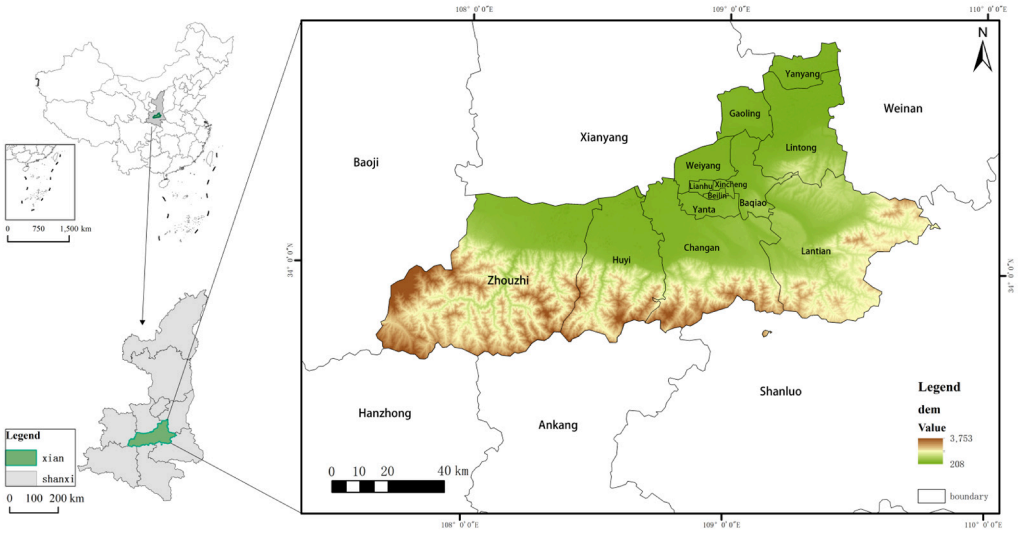


Figure 1. Location of the study area.

2.2. Data Sources and Preprocessing

All data assemblages employed within the present research were classified into five thematic groups: land use, natural environment, socioeconomic status, location and transportation, as well as planning and statistical records. Land-use cartographic datasets for 2000, 2010, and 2020 were adopted to support historical change detection, model calibration, and future scenario projection. These specific years were selected because their data sources, spatial resolutions, and classification schemes are mutually compatible, thereby reducing uncertainties that could stem from inconsistencies in data production and interpretation. Moreover, the 2000–2020 interval captures a critical phase of rapid built-up expansion, widespread cropland conversion, and increasingly stringent ecological protection in Xi'an. Adopting 2020 as the benchmark year also harmonizes the procedures of land-system transition identification, PLUS model validation, MOP-based demand forecasting, and ESV response evaluation. The land-use information was retrieved from the worldwide land-cover 30 global land cover product and subsequently reclassified into six types: cropland, forest land, grassland, water bodies, construction land, and unused land. This reclassified dataset serves as the fundamental spatial input for historical land use analysis, and scenario simulation, as well as ESV assessment [43,44]. Natural environmental variables—encompassing elevation, gradient, thermal conditions, precipitation, aridity, pedological type, and soil erosion type—collectively characterize the study area's geomorphic attributes, hydrothermal patterns, and ecological background constraints. Socioeconomic variables comprise demographic density, regional economic output (GDP), and nocturnal luminosity. The gridded population density together with GDP datasets were obtained via the Resource and Environment Science and Data Center, Chinese Academy of Sciences, while nighttime light records were derived from the VIIRS-DNB annual nighttime light product [45–47]. Location- and transportation-related variables include distances to expressways, primary roads, secondary roads, railways, settlements, and water bodies. For each vector feature (e.g., roads, railways, rivers, residential points, administrative centers), Euclidean distance analysis was performed to generate corresponding distance raster layers.

Prior to model computation, all spatial datasets were standardized using ArcGIS Pro 3.0 (Esri, Redlands, CA, USA). Specifically, the datasets were converted into a unified geospatial reference framework subsequently trimmed to the jurisdictional boundary of Xi'an. The land-system maps were reclassified as six predefined land cover classes described above. Raster layers originating from different source resolutions were regridded onto a consistent 30 m $\times$ 30 m grid, which matches the resolution used for subsequent land use simulation. For vector datasets—such as roads, railways, water networks, settlements, and administrative centers—Euclidean distance analysis was applied to produce distance raster layers. Throughout the model implementation, every raster input was maintained at the 30 m $\times$ 30 m resolution. For cartographic display, certain spatial outputs were aggregated to a 240 m resolution to enhance visual clarity.

3. Research Methods

The methodological framework was organized to link land use demand estimation, spatial allocation simulation, ESV assessment, response analysis, and zoning strategy identification. These procedures support the evaluation of how alternative land use pathways may affect ecosystem service value in Xi'an (Figure 2).

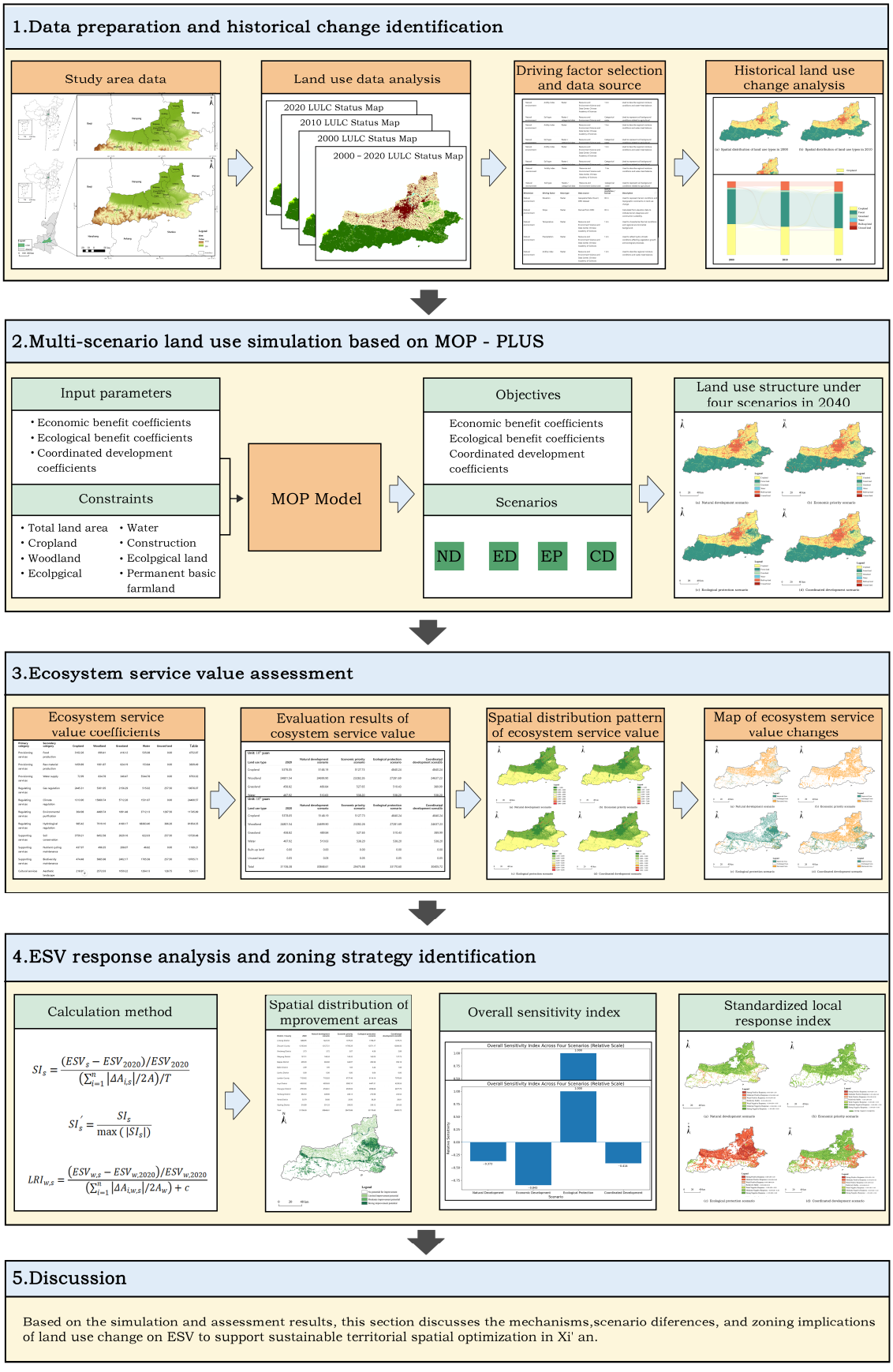


Figure 2. Technical framework of the study.

3.1. Multi-Scenario Land-Use Structure Forecasting Using the MOP Framework

The MOP framework was deployed to estimate the required areal extent of each land-use category within Xi'an contingent on different scenario targets. The optimization allocated total land across six categories by balancing economic output, ecological benefits, and coordinated development objectives while incorporating constraints on total land area, cropland protection, ecological land maintenance, and construction land scale. The resulting land demand provided quantitative inputs for subsequent spatial allocation using the PLUS model. The target year was set to 2040 for three reasons. First, using 2020 as the baseline yields a 20-year projection window, which matches the historical observation period (2000–2020) and enables comparison between past land use trends and future scenario changes. Second, a 2030 projection would be too short after the baseline to clearly differentiate land use structural adjustments, construction land expansion, or ESV responses across scenarios. Third, although 2060 aligns with China's long-term carbon neutrality goal, such a long horizon would involve greater uncertainty in population dynamics, industrial restructuring, policy shifts, and infrastructure development. Thus, 2040 was chosen as a medium- to long-term simulation period with relatively manageable uncertainty. Based on this temporal framework, four scenario pathways were formulated: baseline evolution, economic precedence, ecological conservation, and integrative coordination. The 2040 land-demand estimates generated by the MOP framework were subsequently imposed as quantitative constraints for spatial allocation within the PLUS model.

3.1.1. Construction of Multi-Objective Functions

(1) Economic benefit objective

This objective aims to estimate the economic output arising from alternative land-use allocations. Within the MOP model, its decision variables comprise the areal extents of six land-use types. The aggregate economic benefit is computed as the sum of each land use area multiplied according to its respective standardized economic benefit coefficient per unit area. This objective function can be expressed as follows:

$$\max F_1 = \sum_{i=1}^{6} E_i' x_i \quad (1)$$

in which F_1 represents the economic benefit objective value; x_i denotes the area of the i-th land-use category; E_i' is the standardized economic benefit coefficient assigned to the i-th land-use type; and $i = 1, 2, \ldots, 6$ corresponds to cropland, forest land, grassland, water, construction land, and unused land, respectively.

Based on previous studies [15,48,49], the GM(1,1) model was adopted to estimate the unit-area economic benefit coefficients for 2040 using the values from 2000, 2010, and 2020. Because the coefficient for construction land substantially exceeded those assigned to the remaining land-use categories, directly applying the original predicted values would have made the economic objective dominate the optimization process. To reduce this imbalance, the 2040 coefficients were transformed using ln(x + 1) and then normalized by the min–max method. The standardized coefficient was calculated as follows:

$$E_i' = \frac{\ln(E_i + 1) - \min[\ln(E_i + 1)]}{\max[\ln(E_i + 1)] - \min[\ln(E_i + 1)]} \quad (2)$$

where E_i denotes the original economic benefit coefficient of the i land use type and E_i' represents the standardized value. The standardized coefficients were then introduced into the economic benefit objective function. The economic benefit coefficients of the six land use types are listed in Table 1.

Table 1. Economic benefit coefficients, ecological benefit coefficients, and coordinated development coefficients corresponding to each land use type.

Land Use Type	Cropland	Forest Land	Grassland	Water	Construction Land	Unused Land
Standardized economic benefit coefficient	0.5034	0.1790	0.5302	0.2230	1.0000	0.0000
Standardized ecological benefit coefficient	0.1742	0.6201	0.2573	1.0000	0.0000	0.0307
Coordinated development coefficient	0.3388	0.3996	0.3938	0.6115	0.5000	0.1054

(2) Ecological benefit objective

This objective quantifies the ecosystem service contribution of different land use allocations. Its structure follows that of the economic objective, but the economic benefit coefficient is replaced by a standardized ecological benefit coefficient. The ecological benefit coefficient is derived from the corrected unit-area ESV (ecosystem service value) coefficient for each land use type. Among the six land use categories, forest land and water bodies exhibit higher coefficients, indicating stronger ecosystem service supply capacity. To ensure comparability with the economic objective, the ecological benefit coefficients were standardized prior to incorporation into the MOP model.

(3) Coordinated development objective

The coordinated development objective was designed to represent a balanced allocation between economic output and ecological benefit. Because both the economic and ecological benefit coefficients had been standardized, they could be combined within a unified objective function. In this study, equal weights were assigned to the two objectives, with $\alpha = \beta = 0.5$. This setting defines the coordinated development scenario as a neutral trade-off between the economic priority scenario and the ecological protection scenario. In the context of Xi'an's territorial spatial governance, this assumption reflects the need to consider urban development, cropland preservation, and ecological security simultaneously. The coordinated development coefficient of each land use type was calculated as follows:

$$C_i' = \alpha E_i' + \beta S_i' \tag{3}$$

where C_i denotes the coordinated development coefficient of the i-th land use type; E_i' and S_i' represent the standardized economic and ecological benefit coefficients, respectively, and α and β are the corresponding weights, with $\alpha + \beta = 1$. The coordinated development objective function was then formulated as

$$\max F_3 = \sum_{i=1}^{6} C_i x_i \tag{4}$$

where F_3 represents the coordinated development objective value, and x_i is the area of the i land use type. The coordinated development scenario was obtained by maximizing F_3.

3.1.2. Scenario Setting and Constraint Conditions

Four land use scenarios were established to represent alternative development pathways for Xi'an in 2040: natural development, economic priority, ecological conservation, and integrated coordination. These scenarios were designed to compare how divergent policy orientations may shape land demand and spatial allocation.

The baseline-evolution scenario assumes that land use changes follow the trajectories documented across 2010 and 2020, with land requirements projected by the Markov model under no additional policy interventions. In the economic priority scenario, greater emphasis is assigned to built-up-area enlargement and maximizing economic returns, while still meeting basic requirements for farmland preservation and ecological land protection. The ecological protection scenario gives top priority to maintaining and increasing ecological

land—especially forests, grasslands, and water bodies—and prohibits their conversion into construction land. The coordinated development scenario represents a balanced approach that reconciles the need for construction land with the maintenance of ecological security.

To ensure that MOP outputs align with historical land-use patterns and territorial spatial planning regulations, the decision variables were defined as the areal extents of cropland, forest land, grassland, water, construction land, and unused land. This constraint system was developed by integrating the 2020 land-use baseline, past land-use dynamics, spatial planning mandates, and long-term development flexibility. All area constraints in Table 2 were uniformly expressed in km^2 to avoid unit ambiguity. Constraints comprise aggregate land area, upper and lower thresholds for each land category, a minimum ecological land area, permanent basic farmland protection, and non-negative decision variables. Specifically, the total land area was fixed according to Xi'an's administrative territory. Limits for cropland, forest land, grassland, water, and unused land were established based on their 2020 extents. In particular, the unused land constraint was set at 0.18–0.22 km^2 after unit conversion, accounting for less than 0.01% of the total study area; therefore, it has a limited influence on the overall land-use structure. Construction land was assigned a flexible range to accommodate potential development needs by 2040. The total ecological land area was required to stay at or above 95% of its 2020 level, and permanent basic farmland was maintained as a policy compliance constraint. Detailed constraints are presented in Table 2.

Table 2. Constraint conditions of the MOP model.Simulation of Land-Use Spatial Distribution Based on the PLUS Model.

Item	Constraint Type	Constraints/km^2	Description
1	Total land area constraint	$\sum_{i=1}^{6} x_i = 10,112.00$	The total area of all land-use types is equal to the total area of the study area.
2	Cropland area constraint	$3307.22 \leq x_1 \leq 4042.16$	Cropland is allowed to fluctuate by ±10% relative to its 2020 area, reflecting cropland preservation requirements and moderate adjustment flexibility.
3	Forest land area constraint	$4284.78 \leq x_2 \leq 5236.96$	Forest land is allowed to fluctuate by ±10% relative to its 2020 area, reflecting the need to maintain the stability of ecological space.
4	Grassland area constraint	$180.39 \leq x_3 \leq 244.06$	Grassland is allowed to fluctuate by ±15% relative to its 2020 area, considering its relatively small base area and spatial variability.
5	Water area constraint	$47.34 \leq x_4 \leq 64.06$	Water area is allowed to fluctuate by ±15% relative to its 2020 area, considering hydrological variability and ecological restoration flexibility.
6	Construction land area constraint	$1267.49 \leq x_5 \leq 1830.82$	The lower bound is 10% below the 2020 construction land area, while the upper bound is 30% above the 2020 level, reflecting long-term urban development flexibility toward 2040.
7	Unused land area constraint	$018 \leq x_6 \leq 0.22$	Unused land is allowed to fluctuate by ±10% relative to its 2020 area. Owing to its very small proportion, it has a limited influence on the overall land use structure.

Table 2. *Cont.*

Item	Constraint Type	Constraints/km^2	Description
8	Total ecological land area constraint	$x_2 + x_3 + x_4 \geq 4777.35$	Forest land, grassland, and water are defined as ecological land, and their total area should not be less than 95% of the 2020 level.
9	Permanent basic farmland constraint	$x_1 \geq 901.89$	This policy compliance constraint was set according to permanent basic farmland protection requirements in territorial spatial planning. Although it is not binding under the current cropland lower-bound setting, it is retained to reflect the policy bottom line of cropland protection.
10	Non-negativity constraint of decision variables	$x_i \geq 0, i = 1, 2, \ldots, 6$	All decision variables are non-negative.

Note: x_1–x_6 represent the areas of cropland, forest land, grassland, water, construction land, and unused land, respectively. Ecological land consists of forest land, grassland, and water. All area constraints are expressed in km^2.

3.2. Simulation of Land-Use Spatial Distribution Based on the PLUS Model

In this study, the PLUS model served as the spatial allocation tool following the MOP-based land demand estimation. The model comprises two components: the land expansion-analysis strategy (LEAS) together with the cellular-automata-driven stochastic patch seeding mechanism (CARS). The LEAS module utilizes a random-forest algorithm to estimate the growth potential probability for each land-use category, whereas the CARS module produces future land use patches based on projected demand, neighborhood effects, and transition rules. Using the land demand outputs derived from the MOP framework, the PLUS model was subsequently utilized to reproduce the spatial arrangement of land-use patterns within Xi'an for 2040 under four scenarios: baseline evolution, economic precedence, ecological conservation, and integrated coordination. This workflow connects quantitative land demand forecasting with spatial pattern simulation, providing a basis for assessing medium- to long-term ecosystem service value (ESV) changes after the 2020 baseline.

PLUS model calibration was implemented with the 2010 land-use map, and validation was conducted against the actual 2020 land use pattern. Specifically, land use transition rules and driving factors were applied to reproduce the 2020 spatial distribution, and the model outputs were contrasted against the observed 2020 land-use dataset. After validation accuracy met the modeling requirements, the 2020 land use map was adopted as the baseline for simulating land use patterns under the 2040 scenarios. The selection of driving factors was grounded in the observed land use transitions between 2010 and 2020, Xi'an's physical geography, urban expansion characteristics, and data accessibility. Altogether, 16 driving determinants were incorporated: elevation, gradient, thermal conditions, precipitation, aridity, pedological type, soil-erosion category, population density, GDP, nighttime light index, distance to expressways, distance to main roads, distance to other roads, distance to railways, distance to settlements, and distance to rivers and water bodies. These variables collectively capture natural environmental constraints, socioeconomic development intensity, and location-transportation accessibility. For vector datasets such as roads, railways, settlements, rivers, and water bodies, Euclidean distance analysis was performed to generate distance raster layers. Other continuous raster datasets were processed through projection transformation, clipping, resampling, and standardization. Finally, all driving determinants were regridded to a consistent 30 m × 30 m spatial resolution to conform to the input specifications of the PLUS model.

To elucidate how the driving determinants were integrated into the multi-scenario simulation, they were treated as baseline spatial explanatory variables within the LEAS component within the PLUS framework. These variables were utilized to estimate the expansion probability of each land use type, rather than being adjusted across scenarios. Consequently, all four scenarios shared identical raster layers for natural environment, socioeconomic conditions, and location-transportation factors. Elevation, slope, soil type, and soil erosion type served as relatively stable physical background variables. Temperature, precipitation, and aridity reflected regional hydrothermal regimes. Population density, GDP, and nighttime light index described the spatial intensity of population concentration and economic activity. Distance metrics to roads, railways, settlements, rivers, and water bodies captured accessibility and locational proximity. Prior to model input, all continuous variables were standardized to ensure comparability.

Policy intervention was incorporated into the modeling process through two stages. During the MOP-based demand estimation stage, constraints on total land area, cropland protection, ecological land preservation, permanent basic farmland, and construction land scale defined the allowable quantity ranges for each land-use category across divergent scenarios. During the PLUS-based spatial allocation stage, these policy directions were translated into scenario-specific conversion rules, cost settings, and neighborhood weights within the CARS module. For the natural development scenario, transitions followed the historical trajectory observed from 2010 to 2020. For the ecological-conservation scenario, the allocation favored construction land expansion while retaining minimum requirements for cropland and ecological land. For the baseline-evolution scenario, conversions involving forest, grassland, or water bodies to construction land were prohibited, and the retention or expansion of ecological land was reinforced. For the coordinated development scenario, allocation rules were precluded to balance construction land growth with the preservation of ecological space.

3.3. Ecosystem Service Value Assessment

Ecosystem service value (ESV) assessment translates such ecological impacts of land use change into comparable monetary units. The methodology originates from the ESV framework initially formulated by Costanza et al. and subsequently localized by Xie et al. for China's terrestrial ecosystems. This approach has gained wide application to evaluate regional ecological consequences associated with land-use transition [39,50]. Because each land-use category type provides a different capacity for ecosystem services, variations in land use area can alter aggregate valuation, internal composition, as well as the spatial configuration of regional ESV [50,51]. Given that national-average equivalence factors fail to capture local differences among the Qinling mountain forests, the Weihe River Basin water bodies, and the agricultural areas of the Guanzhong Plain within Xi'an, this study made region-specific adjustments based on Xie et al.'s equivalence value table for China's terrestrial ecosystem services [39,50]. First, the standard equivalence value for the study area was derived using local grain production and grain price data from Xi'an, thereby reflecting regional agricultural productivity and economic value. Second, according to Xi'an's land use classification and natural ecological pattern, the six land use categories were matched with corresponding ecosystem types—cropland, forest land, grassland, water bodies, and unused land. Finally, the per-unit-area ESV coefficient for each land use type was obtained from the adjusted standard equivalence value. This localized calibration enhances the suitability of ESV estimation for Xi'an's ecological conditions while preserving regional comparability [52,53].

ESV was categorized into four primary service types: provisioning, regulating, supporting, and cultural services. These comprise 11 subsidiary services, covering food produc-

tion, material provisioning, water-yield provision, gaseous regulation, climatic regulation, environmental remediation, hydrological modulation, soil retention, nutrient circulation maintenance, biodiversity conservation, and landscape aesthetics (Table 3). The coefficients listed in Table 3 represent the monetized per-unit-area values of ecosystem-service outputs supplied by distinct land-use categories. For construction land, the per-unit-area ESV coefficient was set to zero, following common practice in regional-scale ESV assessments using equivalent factor methods. This treatment is primarily due to the land use classification adopted in this study, where construction land is treated as an aggregated category dominated by artificial surfaces and intensively construction land. Compared with forest, grassland, water bodies, and cropland, this category offers limited capacity to supply ecosystem services at the regional scale. Assigning a zero coefficient to construction land thus avoids overestimating the ecological value of highly artificial land surfaces. However, this does not imply that all ecological spaces within construction land lack ecological value. Urban green spaces, urban water bodies, parks, constructed wetlands, and sponge city facilities may still provide ecological benefits. Nevertheless, given the 30 m spatial resolution and the six-category land use classification, these small-scale blue-green spaces cannot be separately identified within construction land. Consequently, their contribution to ecosystem service value may be somewhat underestimated. Based on the revised per-unit-area ESV coefficients, the total ecosystem service value was calculated as follows:

$$ESV = \sum_{i=1}^{n} A_i \times VC_i \quad (5)$$

where ESV is the total ecosystem service value; A_i is the area of the i land use type; VC_i is the unit area ESV coefficient of the i land use type; and n is the number of land use types.

Table 3. Ecosystem service value coefficients in Xi'an.

Primary Category	Ecosystem Service Value Coefficients in Xi'an/yuan·hm^{-2}·a^{-1}						
	Secondary Category	Cropland	Forest Land	Grassland	Water	Unused Land	Total
Provisioning services	production	3102.26	699.41	416.12	535.08	0.00	4752.87
	Raw material production	1459.89	1601.87	624.19	153.84	0.00	3839.49
	Water supply	72.99	834.78	340.47	5544.78	0.00	6793.02
Regulating services	Gas regulation	2445.31	5301.95	2156.29	515.02	257.50	10,676.07
	Climate regulation	1313.90	15,860.74	5712.26	1531.67	0.00	24,400.57
	Environmental purification	364.98	4489.74	1891.48	3712.13	1287.56	11,745.89
	Hydrological regulation	985.42	7919.10	4180.17	68,383.40	386.26	81,854.35
Supporting services	Soil conservation	3759.21	6452.58	2629.16	622.03	257.50	13,720.48
	Nutrient cycling maintenance	437.97	496.35	208.07	46.82	0.00	1189.21
	Biodiversity maintenance	474.48	5865.98	2402.17	1705.58	257.50	10,705.71
Cultural services	Aesthetic landscape	218.98	2572.03	1059.22	1264.13	128.75	5243.11
Total		14,635.38	52,094.54	21,619.60	84,014.48	2575.09	

3.4. Changes and Response Analysis of Ecosystem Service Value

3.4.1. Overall Sensitivity Index (SI)

The overall sensitivity index (SI) quantifies the responsiveness of ESV to land use change at the regional level. It compares the relative change in ESV against the intensity of land use transitions under a given scenario. A smaller absolute SI value indicates a weaker ESV response to land use alteration. Positive SI values imply that land use transitions enhance ESV, whereas negative values signal a decline. The SI is computed as follows:

$$SI_s = \frac{(ESV_s - ESV_{2020})/ESV_{2020}}{(\sum_{i=1}^{n}|\Delta A_{i,s}|/2A)/T}$$

where SI is the overall sensitivity index for scenario s; ESV_s represents the ecosystem service value under scenario s; ESV_{2020} is the ESV in the baseline year; $\Delta A_{i,s}$ denotes the change in the area of land use type i under scenario s compared with 2020; A is the total area of the study region; T is the length of the study period, and n is the number of land use categories.

Because raw SI values can be influenced by variations in land use change intensity across scenarios, a relative normalization step was subsequently applied. Specifically, the SI value for each scenario was divided by the maximum absolute SI value observed among the four scenarios.

$$SI'_s = \frac{SI_s}{\max(|SI_s|)}$$

where SI'_s denotes the normalized overall sensitivity index under scenario s. After normalization, the direction and relative strength of ESV responses under different scenarios can be compared on the same scale.

3.4.2. Local Response Index (LRI)

The local response index (LRI) was developed to capture the spatial heterogeneity of ESV responses to land use change. Unlike the SI, which describes the overall regional response, the LRI evaluates how ESV changes within local spatial units relative to the intensity of land use transition. In this study, a fixed-size moving window was used as the calculation unit. Within each window, the relative change in ESV and the intensity of land use change were calculated, and their ratio was used to represent the local response strength. The LRI was calculated as follows:

$$LRI_{w,s} = \frac{(ESV_{w,s} - ESV_{w,2020})/ESV_{w,2020}}{(\sum_{i=1}^{n}|\Delta A_{i,w,s}|/2A_w) + c}$$

where $LRI_{w,s}$ is the local response index of window w under scenario s; $ESV_{w,s}$ is the total ESV within window w under scenario s; $ESV_{w,2020}$ is the total ESV within window w in 2020; $\Delta A_{i,w,s}$ is the area change in the i land use type within window w under scenario s; A_w is the total area of window w; and c is a stabilization term introduced to prevent abnormal amplification when land use change intensity is extremely small. Because the original LRI values may vary substantially among scenarios, a robust standardization procedure was applied to make the results comparable. The standardized LRI values were rescaled to the range of $[-1, 1]$, where positive values indicate areas where land use change is associated with ESV improvement, while negative values indicate areas where land use change is associated with ESV decline.

4. Results

4.1. Characteristics of Land Use Change in Xi'an During 2000–2020

Over the period spanning 2000 to 2020, Xi'an maintained a pronounced spatial configuration featuring ecological land within the southern sector, agricultural land across the central-northern plain, and construction land around the urban core (Figure 3). To clarify the main conversion processes, land use transitions for the periods 2000–2010, 2010–2020, and 2000–2020 were analyzed alongside a transfer diagram (Figure 4). At the 2000 baseline, cropland and forest land constituted the two prevailing categories. Cropland was mainly distributed across the plains and tablelands, including Gaoling, Yanliang, Lintong, and the northern parts of Chang'an and Huyi districts. Forest land was predominantly aggregated within the southern Qinling Mountains, particularly in Zhouzhi, Huyi, Chang'an, and Lantian. Construction land was clustered in the central urban districts—Xincheng, Beilin, Lianhu, Yanta, and Weiyang—whereas grassland, water bodies, and unused land appeared

in relatively scattered patches. By 2010, the basic spatial structure remained similar to that of 2000, but construction land had begun to expand around the central urban area and its peripheral zones. This expansion was especially evident in Weiyang, Yanta, Baqiao, and northern Chang'an districts, where some suburban cropland was converted into construction land. By 2020, construction land had extended further outward from the urban core toward Weiyang, Baqiao, northern Chang'an, and western Lintong districts. Cropland was still concentrated in the central-northern plains and tablelands but became increasingly compressed along the urban expansion fringe. Forest land remained stable in the southern Qinling Mountains, indicating that the overall ecological spatial structure experienced only minor changes throughout the observation interval.

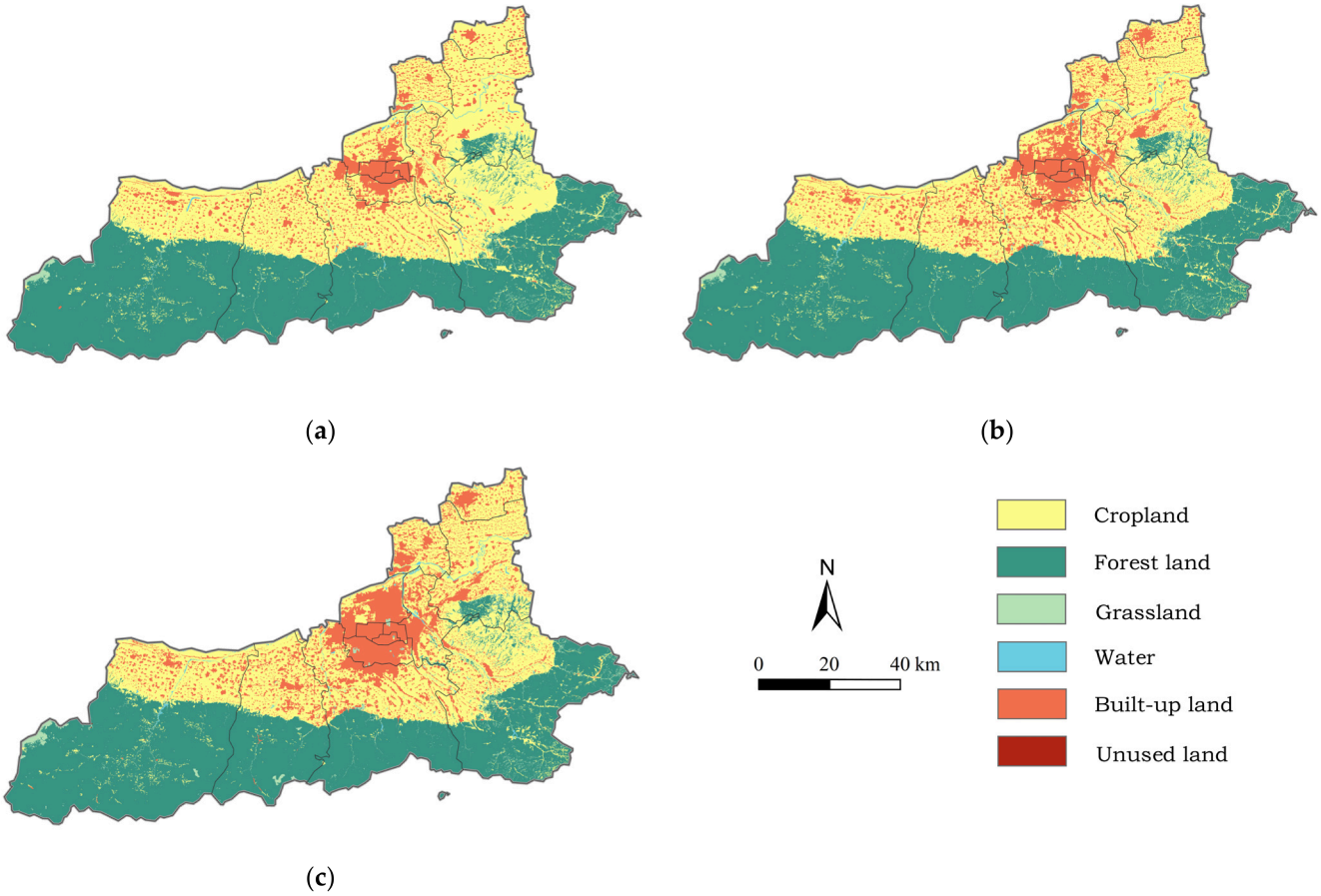


Figure 3. Spatial distribution of land use types in Xi'an from 2000 to 2020. (**a**) Spatial distribution of land use types in 2000; (**b**) spatial distribution of land use types in 2010; (**c**) spatial distribution of land use types in 2020.

This transfer relationship analysis indicates that land use changes in Xi'an from 2000 to 2020 were predominantly driven by interactions among cropland, and forest land, together with construction land (Figure 4 and Table 4). Cropland served as the principal contributor to conversion. Although most cropland patches remained intact, some were converted to construction land, especially in the central-northern plain and suburban expansion zones. This reflects sustained encroachment involving urban growth onto agricultural space during the study period. Construction land exhibited a clear pattern of persistence and outward expansion. In both 2000–2010 and 2010–2020, newly added construction land originated mainly from cropland, indicating that built-up expansion was closely tied to the occupation of peripheral agricultural land around the metropolitan core area as well as adjacent urban clusters. In contrast, forest land remained relatively stable, with only limited

two-way exchanges with cropland while exerting negligible effects on the overall land-use configuration. Grassland, water bodies, and unused land underwent small-scale transitions and had little influence on the overall land use pattern. Overall, land use evolution in Xi'an throughout the 2000–2020 interval was characterized by construction land expansion, cropland reduction, and relative stability of ecological space.

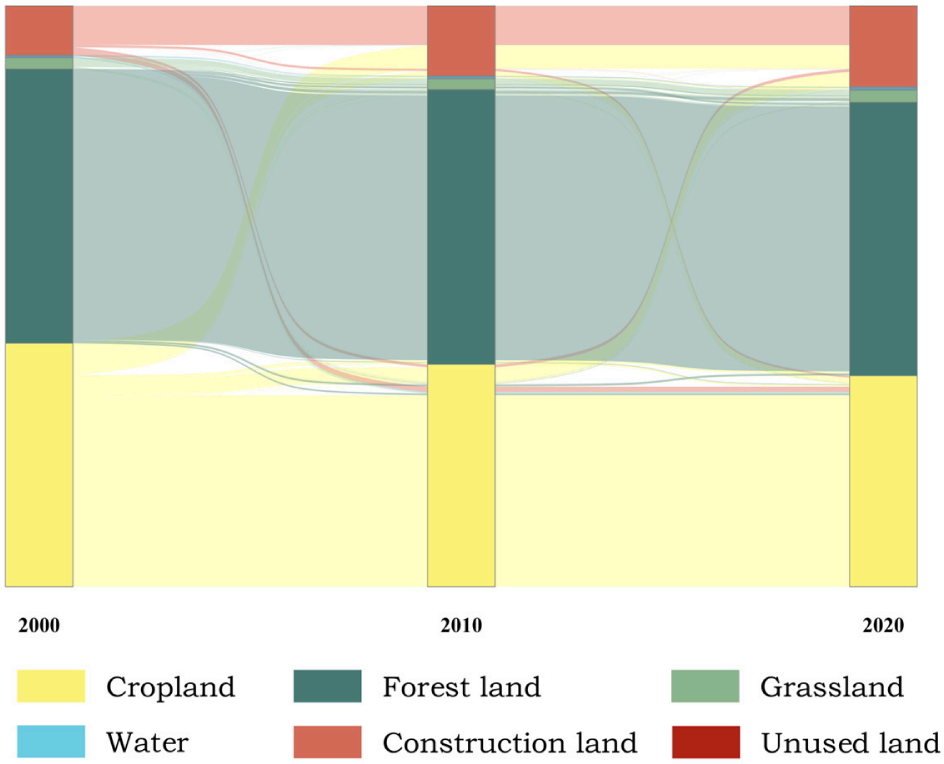


Figure 4. General land use change trends in Xi'an from 2000 to 2020.

Table 4. Area changes in land-use categories in Xi'an during 2000–2020.

Land-Use Category	2000 Area/km^2	2000 Proportion	2010 Area/km^2	2010 Proportion	2020 Area/km^2	2020 Proportion	Change 2000–2010/km^2	Change 2010–2020/km^2	Change 2000–2020/km^2
Cropland	4238.18	41.93%	3872.53	38.31%	3673.39	36.34%	−365.66	−199.13	−564.79
Forest land	4772.89	47.22%	4780.34	47.30%	4758.10	47.08%	7.45	−22.24	−14.79
Grassland	195.18	1.93%	187.25	1.85%	211.93	2.10%	−7.93	24.69	16.76
Water	41.28	0.41%	47.06	0.47%	55.62	0.55%	5.78	8.56	14.34
Construction land	859.87	8.51%	1220.23	12.07%	1408.16	13.93%	360.36	187.93	548.28
Unused land	0.00	0.00%	0.00	0.00%	0.20	0.00% [1]	0.00	0.20	0.20
Total	10,107.40	100%	10,107.40	100%	10,107.40	100%	—	—	—

[1] The proportion of unused land is less than 0.01%; therefore, it is rounded to 0.00% in the table. Note: Positive values indicate area increases, whereas negative values indicate area decreases. Construction land corresponds to built-up land in the original land-use dataset.

4.2. Prediction of Land-Use Composition Across Alternative Scenarios

The estimates summarized in Table 5 present the projected land use composition for Xi'an in 2040 across the four scenarios. The most notable structural shifts are observed in cropland, forest land, and unutilized land, while grassland, water bodies, and unused land exhibit only minor changes. Because unused land occupies less than 0.01% of the total area, its share is rounded to 0.00% in the table. Within the baseline-evolution scenario, construction land expands relative to 1408.32 km^2 in 2020 to 1565.48 km^2, whereas cropland contracts from 3674.69 km^2 to 3517.63 km^2. This implies that, if historical land use trajectories persist, urban expansion will continue to rely primarily on cropland conversion, while forest land remains relatively stable. The economic priority scenario registers the most pronounced growth in construction land, which reaches 1830.82 km^2—an increase of

422.50 km^2 relative to 2020 and the highest among all scenarios. Concurrently, forest land declines to 4469.23 km^2 and cropland to 3503.65 km^2. This pattern suggests that development-oriented expansion heightens pressures on both agricultural land and ecological space. Within the ecological-conservation scenario, forest land expands to 5236.96 km^2, a gain of 476.08 km^2 compared with 2020, while construction land shrinks to 1267.49 km^2. This reflects a strong emphasis on preserving ecological land and restraining built-up expansion. Within the integrated-coordination scenario, construction land attains an equivalent extent as in the economic priority scenario, yet forest land remains substantially higher. This indicates that the coordinated development pathway maintains a relatively large ecological land area even under high construction land demand. Nevertheless, given the continued intensity of construction land expansion, the ecological performance of this scenario should be further interpreted in conjunction with the subsequent ESV and response index results.

Table 5. Prediction of land use structure under different scenarios.

Land-Use Category	2020 Land-Use Status		Natural Development Scenario		Economic Priority Scenario		Ecological Protection Scenario		Coordinated Development Scenario	
	Area/km^2	Proportion	Area/km^2	Proportion	Area/km^2	Proportion	Area/km^2	Proportion	Area/km^2	Proportion
Cropland	3674.69	36.34%	3517.63	34.79%	3503.65	34.65%	3307.22	32.71%	3307.22	32.71%
Forest land	4760.87	47.08%	4741.36	46.89%	4469.23	44.20%	5236.96	51.79%	4729.33	46.77%
Grassland	212.23	2.10%	226.57	2.24%	244.06	2.41%	236.10	2.33%	180.39	1.78%
Water	55.70	0.55%	60.78	0.60%	64.06	0.63%	64.06	0.63%	64.06	0.63%
Construction land	1408.32	13.93%	1565.48	15.48%	1830.82	18.11%	1267.49	12.53%	1830.82	18.11%
Unused land	0.20	0.00% [1]	0.18	0.00% [1]	0.18	0.00% [1]	0.18	0.00% [1]	0.18	0.00% [1]
Total	10,112.00	100%	10,112.00	100%	10,112.00	100%	10,112.00	100%	10,112.00	100%

[1] The proportion of unused land is less than 0.01%; therefore, it is rounded to 0.00% in the table. Note: The land-use categories refer to the six reclassified types used in this study: cropland, forest land, grassland, water, construction land, and unused land.

4.3. Results of Land-Use Spatial Distribution Simulation Based on the PLUS Model

Prior to projecting the projected 2040 land use pattern, the PLUIS framework was calibrated and validated with a historical land-use map, together with selected explanatory determinants, which were employed to reproduce the 2020 land-use configuration, and the simulated output was compared with the observed 2020 map. The validation yielded an overall accuracy of 89.16% with a Kappa coefficient of 0.823, denoting strong agreement between the reproduced simulated and observed patterns. Consequently, the validated PLUIS model was adopted for the subsequent 2040 scenario simulations.

Using the 2020 land use map as the initial condition, this study projected the 2040 land-use configuration across four scenarios: baseline evolution, economic precedence, ecological conservation, and integrated coordination; economic priority, ecological protection, and coordinated development (Figure 5). The fundamental territorial structure of Xi'an was preserved across all scenarios: forest land remained aggregated within the southern Qinling Mountains, cropland dominated the central-northern plains and tablelands, as well as construction land clustered around the central urban area. However, the scenarios diverged with respect to built-up land expansion intensity and ecological space continuity. Within the baseline-evolution scenario, construction land expanded outward from the central urban districts—including Xincheng, Beilin, Lianhu, Yanta, and Weiyang—extending further toward the northern Chang'an District, Baqiao District, as well as western Lintong District. The economic priority scenario exhibited more pronounced expansion, with additional construction land patches emerging not only along the central urban fringe but also in northern Chang'an District, Baqiao District, western Lintong District, and northern Huyi District. This expansion intensified pressures on adjacent cropland and local ecological land. Under the ecological protection scenario, forest land continuity within the southern Qinling Mountains was reinforced, particularly in southern Zhouzhi County, Huyi District, Chang'an District, and Lantian County. Ecological land also expanded in the piedmont

transition zone, while construction land expansion was effectively constrained. In the coordinated development scenario, construction land remained concentrated within the metropolitan core and its peripheral expansion zones, whereas the forest land pattern in the southern Qinling Mountains was generally preserved. This scenario thus reflected a spatial allocation pattern where relatively high construction land demand coexisted with the protection of major ecological space.

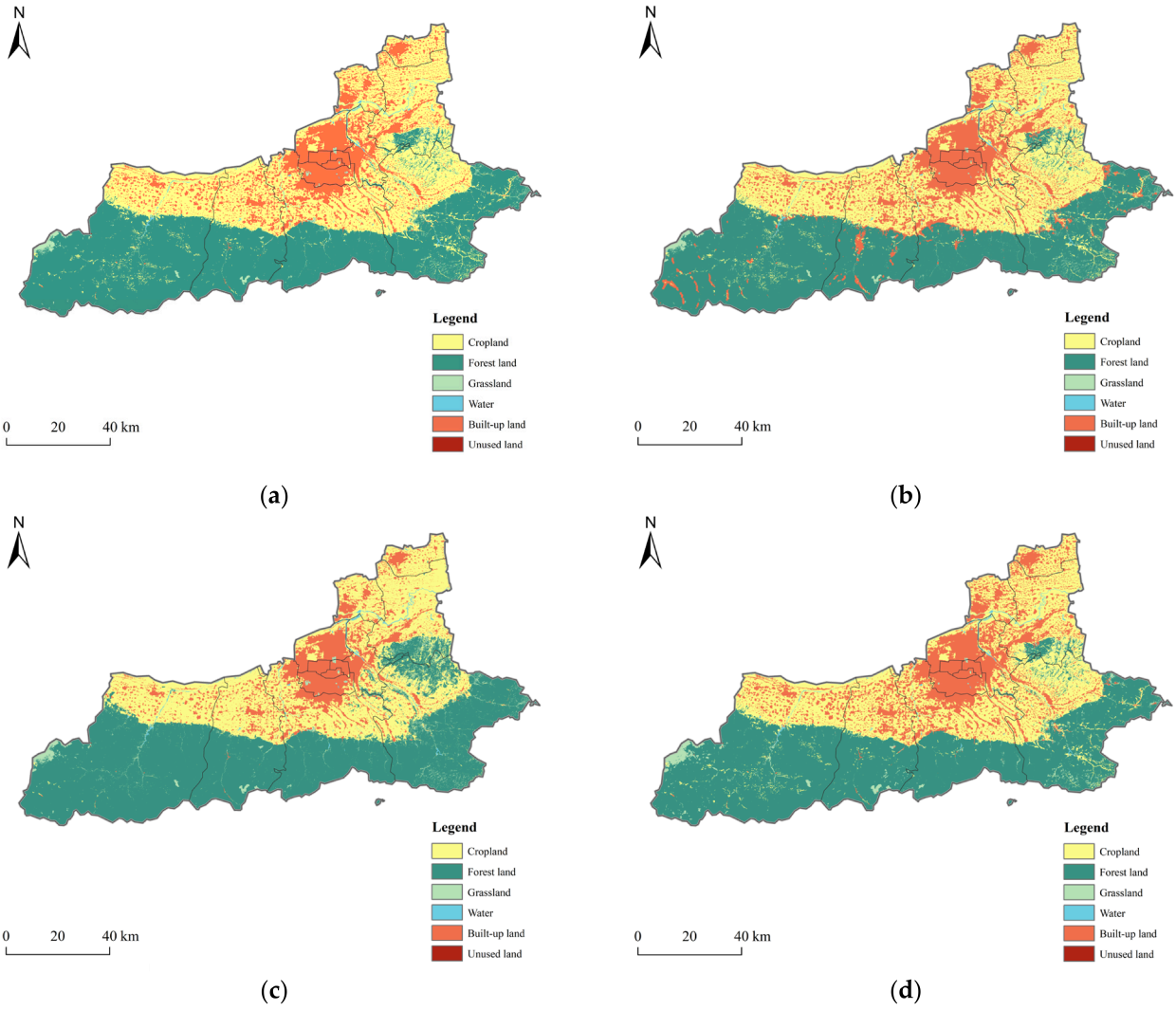


Figure 5. Spatial simulation of land use distribution under different scenarios. (**a**) Natural development scenario; (**b**) economic priority scenario; (**c**) ecological protection scenario; (**b**) coordinated development scenario.

4.4. Ecosystem Service Assessment Results

Drawing on the 2020 land-use configuration and the projected 2040 land-use allocations, ESV was calculated for the baseline year and the four future scenarios (Table 6, Figure 6). The 2040 results were benchmarked against the 2020 baseline to assess how different development pathways might affect the spatial variation in ESV. Figure 7 maps the ESV variations relative to the 2020 baseline.

Table 6. Results of Ecosystem Service Value Assessment.

Land-Use Category	Evaluation Results of Ecosystem Service Value/10^6 yuan				
	2020	Natural Development Scenario	Economic Priority Scenario	Ecological Protection Scenario	Coordinated Development Scenario
Cropland	5378.05	5148.19	5127.73	4840.24	4840.24
Forest land	24,801.54	24,699.90	23,282.26	27,281.69	24,637.23
Grassland	458.82	489.84	527.65	510.43	389.99
Water	467.92	510.63	538.20	538.20	538.20
Construction land	0.00	0.00	0.00	0.00	0.00
Unused land	0.05	0.05	0.05	0.05	0.05
Total	31,106.38	30,848.61	29,475.88	33,170.60	30,405.72

Note: The unit of ESV is 10^6 yuan. The land-use categories refer to the six reclassified types used in this study: cropland, forest land, grassland, water, construction land, and unused land. Construction land was assigned an ESV coefficient of zero under the regional-scale equivalent factor method adopted in this study.

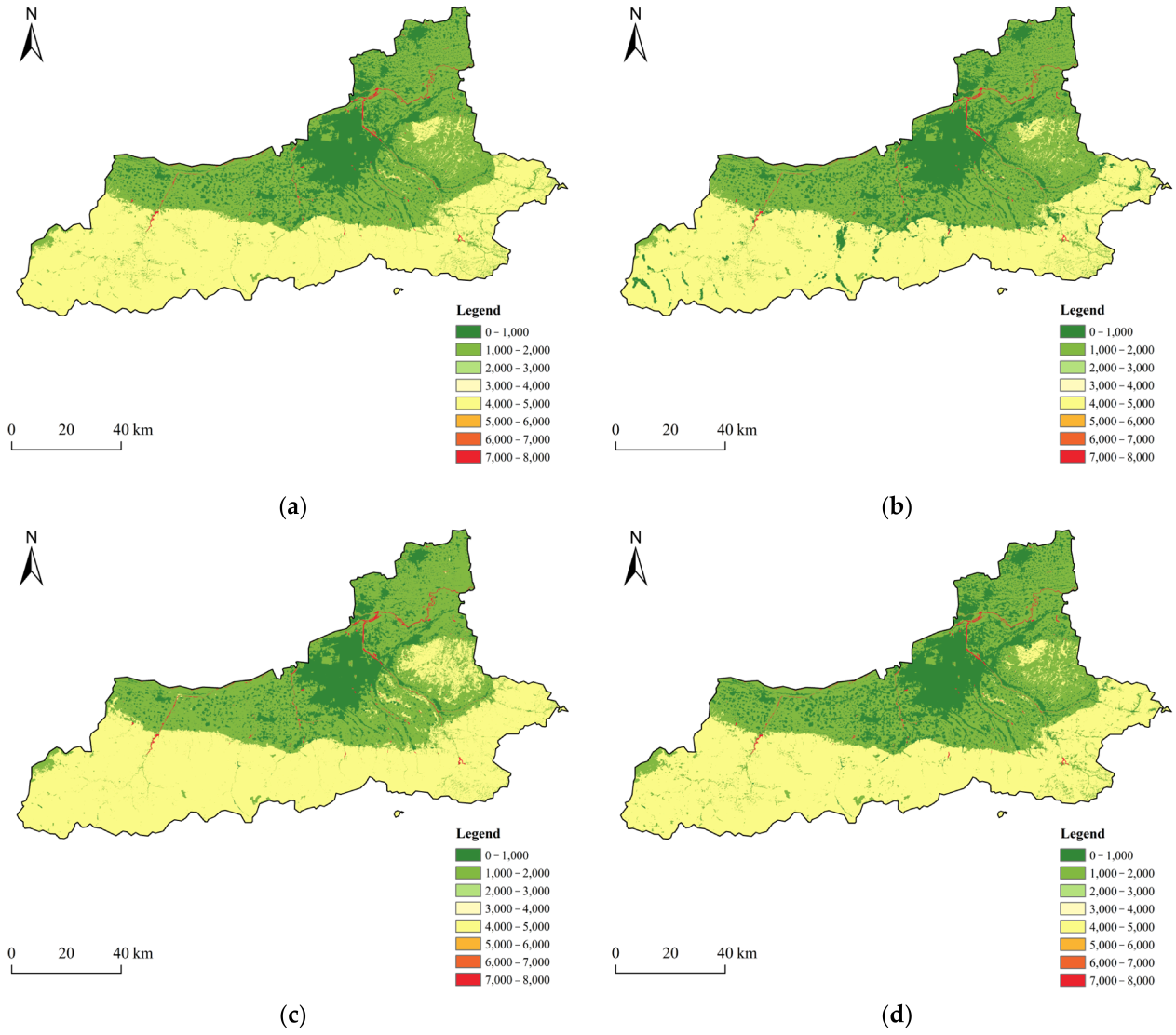


Figure 6. Spatial distribution pattern of ecosystem service value in Xi'an under different scenarios. (**a**) Natural development scenario; (**b**) economic priority scenario; (**c**) ecological protection scenario; (**d**) coordinated development scenario.

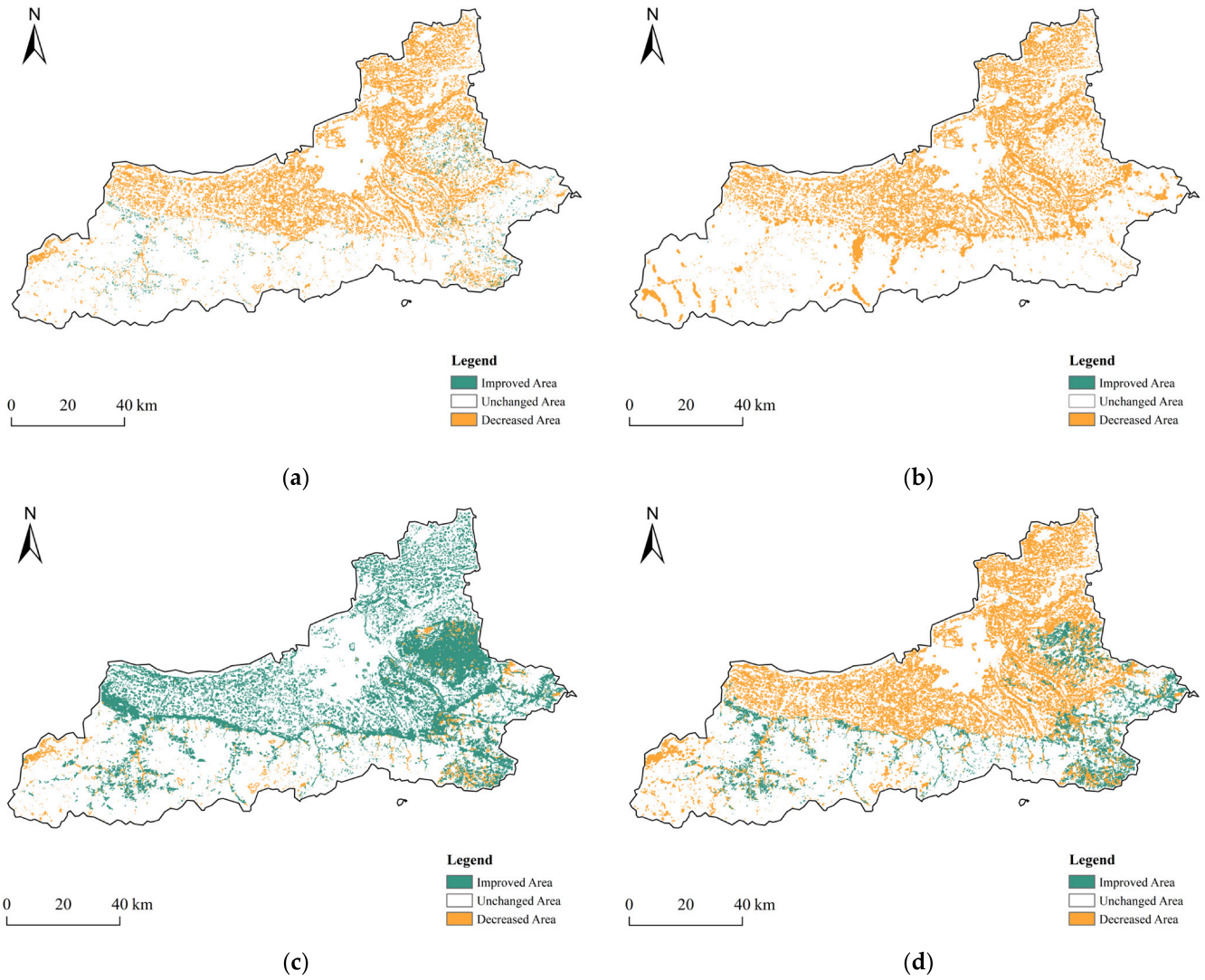


Figure 7. Spatial distribution of changes in ecosystem service value in Xi'an under different scenarios relative to 2020. (**a**) Natural development scenario; (**b**) economic priority scenario; (**c**) ecological protection scenario; (**d**) coordinated development scenario.

The aggregate ESV for Xi'an in 2020 was 31,106.38 × 10^6 yuan. The four scenarios yielded divergent ecological outcomes. The ecological protection scenario produced the highest ESV, reaching 33,170.60 × 10^6 yuan—a 6.64% increase over the 2020 level. Conversely, the economic priority pathway showed the minimum ESV, amounting to 29,475.88 × 10^6 yuan, corresponding to a 5.24% decline. The natural development and coordinated development scenarios recorded ESVs of 30,848.61 × 10^6 yuan and 30,405.72 × 10^6 yuan, respectively, representing decreases of 0.83% and 2.25%. From a land-use contribution perspective, forest land remained the dominant source of regional ESV. In 2020, it contributed 24,801.54 × 10^6 yuan, accounting for 79.7% of the total. Cropland was the second-largest contributor, while grassland and water bodies contributed smaller shares. Because the unit-area ESV coefficient assigned to construction land was set to zero under the regional-scale equivalent factor approach, construction land did not directly contribute to the calculated ESV.

As illustrated in Figure 6, ESV across Xi'an displays a marked north–south differentiation across all four scenarios, though the continuity and extent among high- and low-value zones vary by scenario. Within the natural development pathway, areas with elevated ESV are predominantly located within the southern Qinling Mountains, covering southern

Zhouzhi, Huyi, Chang'an, and Lantian. Low-ESV zones occur predominantly within the metropolitan core as well as adjacent construction land clusters. In the economic priority scenario, low ESV zones expand further across the central region and urban growth areas, particularly along the central urban fringe, Weiyang, Baqiao, northern Chang'an, and western Lintong districts. This spatial pattern reflects a weakening of local ecosystem service supply driven by intensified construction land expansion. The ecological-conservation pathway presents a different pattern: the southern Qinling Mountains remain the core high-value ESV area, and high-value patches become more interconnected in the piedmont transition zone and ecological land expansion areas. This indicates that forest land protection and ecological land expansion can enhance regional ESV. In the coordinated development scenario, high-value zones in the southern Qinling Mountains remain relatively stable, whereas the central construction land clusters still display low-value characteristics. Overall, this scenario reflects the coexistence of major ecological space stability with continued construction land expansion.

Figure 7 further illustrates the spatial configuration of ESV changes relative to the baseline-year baseline. Under the natural development scenario, most areas remain stable, with ESV declines scattered primarily around the central urban fringe and the central–northern expansion zones. ESV increases are limited, implying that continuing historical land use trends would produce only modest ecological effects. In the economic priority scenario, ESV losses become more pronounced and are concentrated along the central urban periphery, in Weiyang, Baqiao, northern Chang'an, and western Lintong, as well as portions of the central–northern plain. This pattern indicates that construction land expansion would diminish ecosystem service provision in urban growth areas. Under the ecological protection scenario, ESV gains are more extensive and are predominantly situated within the southern Qinling Mountains, the piedmont transition zone, and local ecological land expansion areas. This outcome suggests that forest land expansion and ecological space protection can enhance regional ESV. In the coordinated development scenario, both ESV gains and losses are observed. Local increases occur predominantly in the southern ecological areas, while declines remain concentrated in the central–northern construction expansion zones. This reflects the persistent spatial trade-off between urban development and ecological protection under this scenario.

4.5. Identification and Analysis of Ecosystem Service Improvement Areas Under a Sustainable Development Orientation

To identify where ESV could be improved through land use adjustment, this study analyzed ESV changes at two spatial scales: district/county units and pixels. At the district/county scale, total ESV and its changes were compared between the 2020 baseline and the 2040 scenarios (Table 7). At the pixel scale, the maximum positive ESV change for each pixel was extracted from the four scenario-based ESV change rasters. This procedure was used to locate areas where land use adjustment may generate ecological benefits. For map readability, the potential improvement raster was aggregated to 240 m. Pixels with positive ESV change values were then classified using the quantile method. Four categories were identified: high improvement potential, moderate improvement potential, limited improvement potential, and no improvement potential (Figure 8). This classification provides a spatial basis for identifying priority areas for ecological restoration and territorial spatial regulation.

Table 7. Results of Ecosystem Service Value Assessment at the District and County Scale.

District/County	Evaluation Results of Ecosystem Service Value at the District and County Scale/10^6 yuan				
	2020	Natural Development Scenario	Economic Priority Scenario	Ecological Protection Scenario	Coordinated Development Scenario
Lintong District	1488.95	1447.25	1379.23	1768.27	1379.72
Zhouzhi County	12,163.44	12,127.21	11,785.29	12,571.17	12,004.50
Xincheng District	3.73	3.72	3.07	4.56	2.89
Weiyang District	157.31	148.24	145.32	162.05	137.75
Baqiao District	405.59	383.60	344.97	493.58	356.18
Beilin District	2.09	1.95	1.83	2.44	1.68
Lianhu District	0.00 [1]	0.00 [1]	0.00 [1]	0.00 [1]	0.00 [1]
Lantian County	7139.62	7102.63	6737.46	8114.14	7070.69
Huyi District	4339.02	4305.83	3982.10	4447.31	4239.55
Chang'an District	4793.65	4746.61	4530.04	4958.66	4677.79
Yanliang District	262.32	249.66	246.13	272.98	232.52
Yanta District	33.79	30.60	23.50	36.29	20.81
Gaoling District	316.89	301.33	296.93	339.12	281.65
Total	31,106.38	30,848.61	29,475.88	33,170.60	30,405.72

[1] Due to the extremely small area of ecological land in Lianhu District, its ESV is approximately 0 under some scenarios.

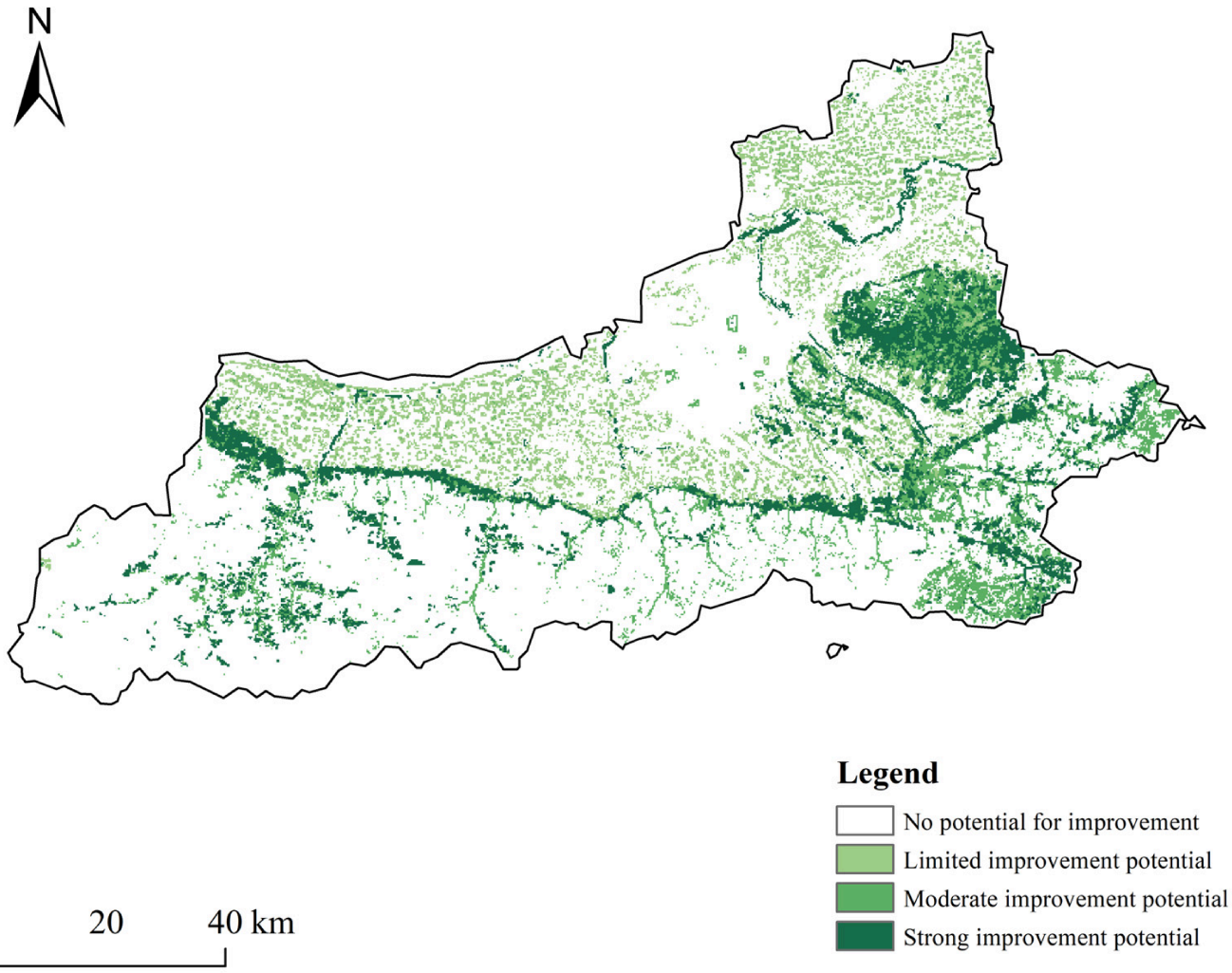


Figure 8. Spatial distribution map of ecosystem service improvement areas in Xi'an.

At the district/county scale, ESV showed clear spatial differences across Xi'an (Table 7). In 2020, elevated ESVs were predominantly concentrated in Zhouzhi, Lantian, Chang'an, and Huyi. These administrative units are located within or near the Qinling Mountains and the piedmont transition zone, where forest resources are abundant and the ecological background is relatively favorable. They therefore formed the main contribution areas of regional ESV, with Zhouzhi County showing the highest value. By contrast, the central urban districts, namely Xincheng, Beilin, Lianhu, Yanta, and Weiyang, had lower total ESV. This was closely associated with the substantial share of construction land alongside the scarcity of ecological land in these districts. Within the ecological-conservation pathway, most districts, as well as counties showed ESV increases, with particularly evident improvements in Lantian, Chang'an, Huyi, as well as Chang'an District. This suggests that ecological protection measures are more effective in the southern mountainous areas and piedmont zones. Under the economic priority scenario, ESV declined in most districts and counties, especially in Lantian County, Chang'an District, Huyi District, and Baqiao District. This indicates that construction land expansion would weaken ecosystem service functions in these areas. Under the coordinated development scenario, the ESVs of most districts and counties were generally between those of the natural development and economic priority scenarios, reflecting an intermediate pattern between development demand and ecological protection.

From the spatial distribution of ecosystem service improvement potential (Figure 8), Xi'an shows clear characteristics of clustered areas and corridor-like patterns in terms of improvement potential. High improvement potential areas are mainly concentrated in Lantian County in the southeast and the piedmont transition zone in southeastern Chang'an District, with relatively continuous patches also formed in southeastern Baqiao District, southern Lintong District, and some eastern local areas. This indicates that these areas have a favorable ecological restoration basis and considerable potential for ecosystem service enhancement. Moderate improvement potential areas are mostly distributed around the periphery of high-potential areas and extend in a belt-like pattern along the northern piedmont zone of the Qinling Mountains, river corridors, and some low-mountain and hilly areas. This reflects the potential for ecological land expansion and landscape connectivity restoration. Limited improvement potential areas are widely and sporadically distributed in the central-northern plain areas and suburban transition zones, mainly appearing as small-scale patchy improvement spaces. In contrast, the central urban area and most built-up areas generally show no improvement potential, indicating that highly urbanized areas are constrained by the existing land use pattern and have relatively limited space for improving ecosystem services.

4.6. Response Evaluation of Ecosystem-Service Value Responses to Land-Use Transition

To distinguish regional-level sensitivity from local spatial response, this study applied the overall sensitivity index (SI) and local response index (LRI). SI was used to compare the direction and intensity of ESV response across scenarios at the regional scale, whereas LRI was used to map local response direction, response strength, and spatial heterogeneity (Figures 9 and 10).

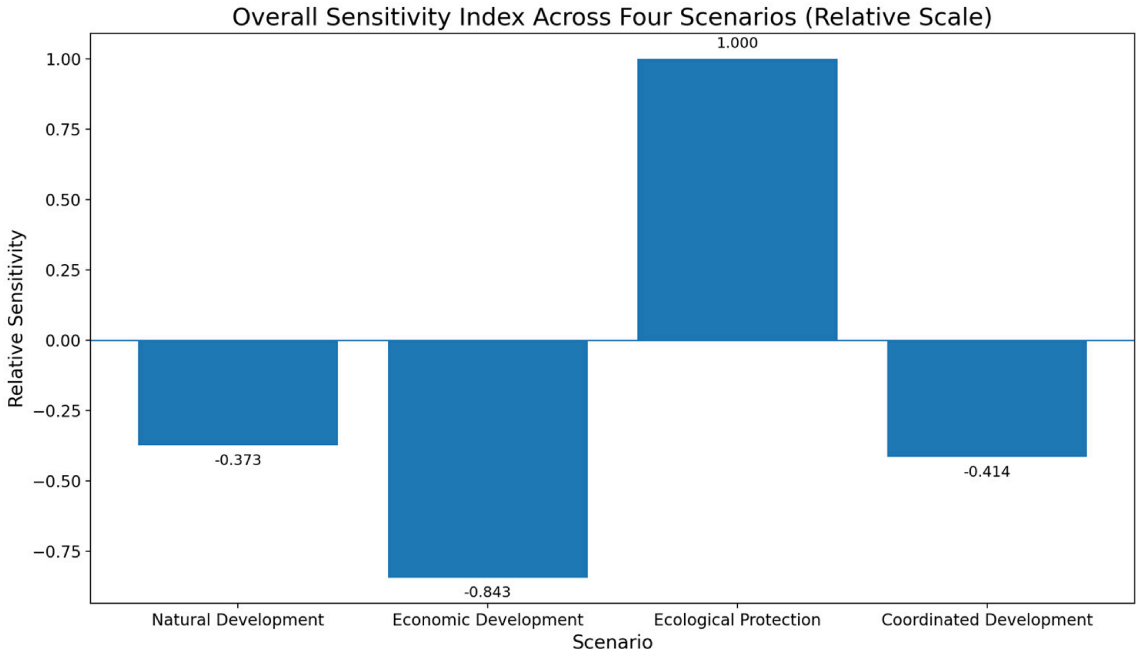


Figure 9. Comparison of the overall sensitivity index in Xi'an under different scenarios.

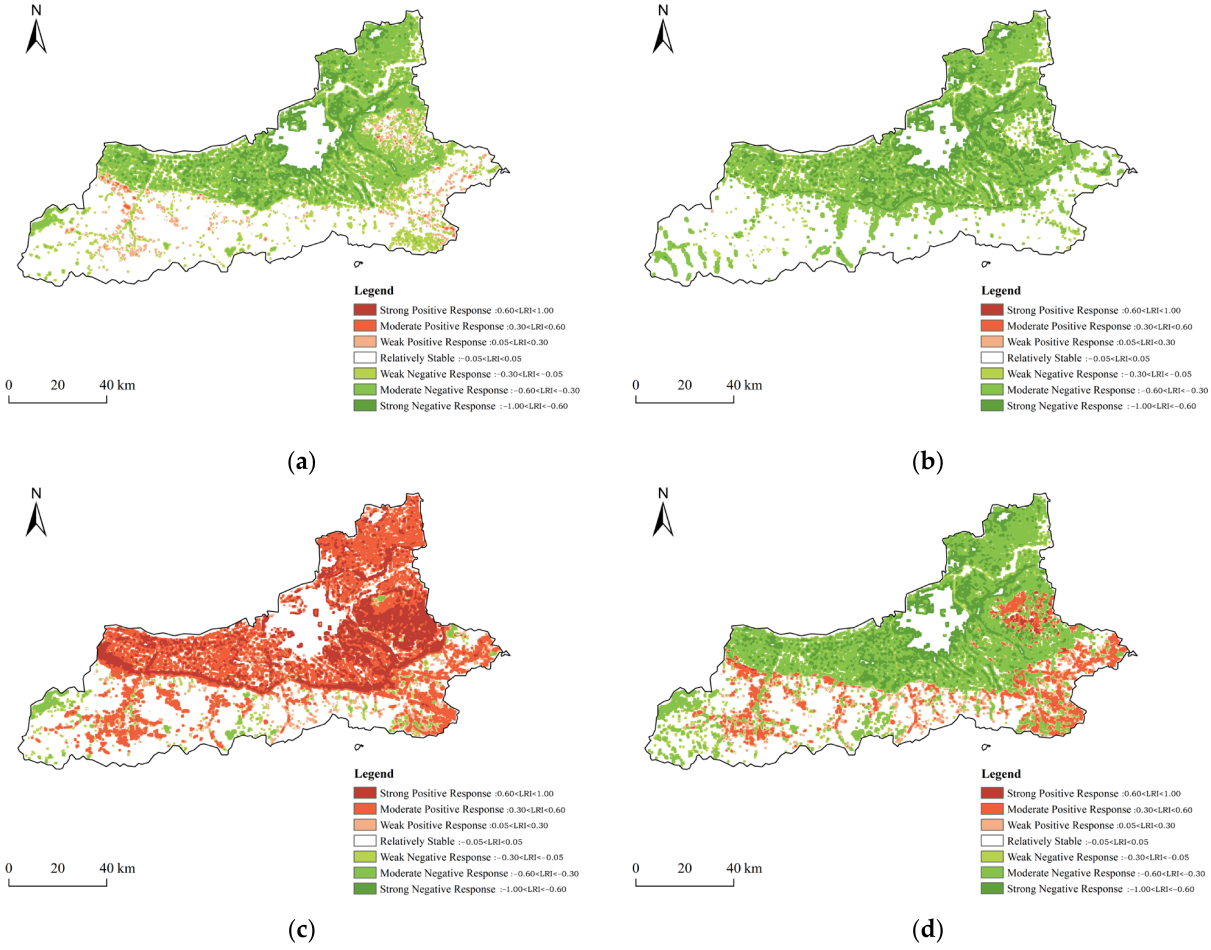


Figure 10. Spatial distribution of the standardized local response index in Xi'an under different scenarios. (**a**) Natural development scenario; (**b**) economic priority scenario; (**c**) ecological protection scenario; (**d**) coordinated development scenario.

The SI results reveal clear scenario differences. The ecological-conservation pathway obtained the maximum relative SI magnitude, reaching 1.00, while remaining the only scenario with a positive SI. This suggests that ecological protection-oriented land use adjustment can enhance regional ESV. Conversely, the economic priority pathway recorded the minimum SI value, amounting to −0.843, indicating the strongest negative response. This means that construction land expansion and ecological land compression under an economically oriented pathway would reduce regional ecosystem service value. The natural development and coordinated development scenarios had SI values of −0.373 and −0.414, respectively. Although both values were negative, their response intensities were weaker than that of the economic priority scenario. Therefore, ESV would still decline under these two scenarios, but the decline would be relatively limited. Overall, ecological protection produced the strongest positive ESV response, while economic priority generated the most pronounced negative response.

To further identify local ESV response patterns, the standardized LRI results were mapped for the four scenarios (Figure 10). Under natural development, negative responses occupied a broad spatial extent. Weak, moderate, and strong negative responses appeared in the southern Qinling Mountains, the central–northern plain, and the piedmont transition zone. Positive responses were limited and occurred only in scattered areas in the southwest, southeast, and some suburban fringes. This pattern implies that the continuation of historical land use trends would generally reduce local ESV. The economic priority scenario showed the widest distribution of negative responses. Strong and moderate negative responses extended across the southern Qinling Mountains and most central–northern areas, while positive response patches were sparse and fragmented. This indicates that an economic-oriented pathway would intensify local ecosystem service losses. The ecological protection scenario displayed a different spatial pattern, with positive responses becoming more evident. Strong and moderate positive responses were located mainly in the northern plain, the northern piedmont zone of the Qinling Mountains, Lantian County, and southeastern Chang'an District, where continuous patches emerged in some mountain–plain transition areas. This result suggests that ecological protection and ecological land expansion are associated with stronger positive ESV responses at the local scale. In the coordinated development scenario, positive and negative responses occurred simultaneously, indicating clear spatial differentiation. Positive responses were located mainly in southeastern Lantian County, southeastern Chang'an District, and parts of the piedmont transition zone. Negative responses appeared primarily in the northern plain, the central urban fringe, and construction expansion zones. This suggests that ecological land improvement can generate local ESV gains under this scenario, but continued construction land expansion may still lead to ecosystem service losses in some areas.

5. Discussion

5.1. Methodological Contributions and Innovations of the Research Framework

Rather than treating model integration as the main contribution, this study emphasizes how land use simulation results can be translated into ESV response interpretation and territorial spatial governance implications. The proposed framework links three analytical steps that are often treated separately: estimating land use demand, allocating land use patterns spatially, and identifying the regional and local responses of ESV. By connecting MOP-based quantity optimization with PLUS-based spatial simulation, the study reduces the gap between land use demand estimation and spatial allocation. By combining ESV assessment with SI and LRI, it further extends the analysis from total value comparison to spatial response identification. Finally, the scenario results are interpreted in relation to

ecological protection, cropland preservation, and construction land expansion, providing a basis for zoning-oriented governance recommendations.

(1) The MOP model calculates the required area for each land use type across the economic-precedence, ecological-conservation, and integrated-coordination pathways. Such optimized area demands are then fed into the PLUS model, which produces spatial land use patterns by applying conversion rules, driving factors, and patch-generation mechanisms. Through this integrated process, the study moves beyond merely projecting the total land demand by 2040 and begins to explore where different land-use categories are projected to be located under alternative future scenarios.

(2) The use of SI and LRI shifts the ESV analysis from aggregate comparison to response-based interpretation. Scenario-based ESV studies often focus on whether total ESV increases or decreases under alternative land use patterns. Such a comparison is useful for evaluating overall ecological outcomes, but it provides limited information on how sensitively ESV responds to land use change and where positive or negative responses occur. In this study, SI was used to compare the regional response direction and intensity of ESV across scenarios, while LRI was used to identify spatial heterogeneity in local ESV responses. This analytical extension makes it possible to distinguish not only which scenario produces the highest or lowest total ESV, but also which areas show improvement potential and which areas are more vulnerable to construction land expansion.

(3) At the administrative-unit level, Zhouzhi County, Lantian County, Chang'an District, and Huyi District were identified as the core areas supporting ESV. At the pixel level, the results of improvement-potential analysis pinpointed priority zones for ecological enhancement, including the northern piedmont zone of the Qinling Mountains, Lantian County, and southeastern Chang'an District. This cross-scale evidence moves the analysis beyond city-wide ESV comparisons toward location-specific governance insights. It suggests that Xi'an's territorial spatial regulation should adopt differentiated strategies, including ecological protection of the Qinling Mountains, cropland control in the Guanzhong Plain, ecological compensation within built-up districts, and restoration of the piedmont transition zone.

5.2. Sustainable Development Implications of Land-System Reconfiguration Across Alternative Pathways

The cross-scenario comparison offers different insights for future land use governance in Xi'an. Quantitatively, the four pathways produced clear differences in both land-use structure and ESV outcomes. Construction land expanded most strongly under the economic-priority scenario, reaching 1830.82 km^2 in 2040, whereas it was constrained to 1267.49 km^2 under the ecological–conservation pathway. This indicates a substantial divergence in urban expansion intensity across scenarios. In terms of ecological outcomes, the ecological-conservation pathway generated the highest total ESV, reaching 33,170.60 $\times$ 10^6 yuan, which was 6.64% higher than the 2020 baseline. By contrast, the economic-priority scenario produced the lowest total ESV, at 29,475.88 $\times$ 10^6 yuan, representing a 5.24% decrease. The ESV gap between these two pathways reached 3694.72 $\times$ 10^6 yuan, demonstrating that alternative land-use pathways can lead to pronounced differences in ecosystem service outcomes. These quantitative contrasts further confirm that controlling construction land expansion while maintaining forest land and other ecological spaces is essential for sustaining regional ESV. Within the baseline-evolution pathway, historical land use inertia would persist, with construction land expanding and both cropland and ecological land facing further shrinkage. This implies that, without active spatial regulation, unguided urban growth may gradually erode regional

ecosystem service supply. The economic priority scenario exhibited the most intensive construction land expansion and the largest decline in total ESV. This pattern suggests that an economic-growth-oriented pathway could increase land development intensity but would also exacerbate ecosystem service losses and undermine long-term regional sustainability. Conversely, the ecological-conservation pathway increased forest land and other ecological land, yielding the maximum aggregate ESV across the four pathways. This outcome highlights the pivotal role of ecological space expansion in strengthening ecological security and ecosystem service provision. However, construction land growth was more strictly constrained in this scenario, indicating a persistent trade-off between ecological conservation and urban expansion. The integrated-coordination pathway represented an intermediate pathway between economic growth and ecological protection. Although it did not fully prevent ESV decline, it maintained a relatively larger ecological land area under high construction land demand. Therefore, future land use transformation in Xi'an should move away from a single expansion-oriented logic and shift toward integrated regulation that balances development demand, ecological protection, cropland preservation, and spatial efficiency.

5.3. Mechanisms Linking Land-System Transition and ESV Responsiveness

The responsiveness of ESV to land-system transition is primarily governed by the ecological functions inherent to each land-use category as well as its spatial arrangement. Forest land, herbaceous land, and aquatic areas typically deliver stronger regulating, supporting, and cultural services, whereas cropland contributes to food production and certain ecological functions. In contrast, construction land offers a limited contribution within the regional-scale ESV accounting framework adopted in this study. Consequently, expanding ecological land, protecting forest land and water bodies, and enhancing ecological connectivity tend to increase regional ESV. Conversely, when construction land encroaches upon cropland and ecological space, the overall supply of ecosystem services may decline.

The scenario results from Xi'an support this mechanism. The ecological protection scenario increased forest land and strengthened ecological spatial continuity, thereby raising ESV in the Qinling Mountains and the piedmont transition zone. The economic priority scenario led to rapid construction land expansion and compression of cropland and ecological land, which weakened the regional ecosystem service supply. The natural development scenario maintained the historical land use trajectory, resulting in inertial construction land growth and only modest ecological improvement. The coordinated development scenario reflected a pragmatic compromise under multiple spatial constraints, yet it still showed that ecological benefits may diminish when construction terrain unit demand remains high. These findings indicate that the influence of land-system transition on ESV depends not only on the area of land converted but also upon the type, location, and ecological function of the converted land. For Xi'an, enhancing regional ESV requires more than simply increasing ecological land area. It also entails controlling construction land expansion along sensitive agricultural–urban interfaces, preserving the continuity of the Qinling ecological space, and strengthening ecological connectivity in the piedmont transition zone and urbanized districts.

Viewed through a spatial-heterogeneity lens, the ESV responsiveness within Xi'an is shaped by the functional division among southern ecological space, central urban construction space, and northern agricultural space. The southern Qinling Mountains, where forest land is concentrated, provide the primary ecological foundation for regional ESV. Therefore, the stability of forest land and the effectiveness of ecological protection in this area exert a decisive influence on the citywide ESV level. In contrast, the central urban area and surrounding construction expansion zones exhibit relatively low ESV due to the high

proportion of construction land and limited ecological space. These areas are thus more susceptible to ecosystem service losses. In the northern plain, where cropland is widely distributed, land use change mainly affects food provision and certain regulating services.

Overall, Xi'an displays a composite spatial pattern in which the southern mountains supply ecological support, the central urban area generates continuous disturbance, and the northern agricultural space remains under dynamic adjustment. The SI and LRI results further indicate that ESV responses differ between regional and local scales. At the regional scale, ecological protection yields the strongest positive response, whereas economic priority produces the most pronounced negative response. At the local scale, the piedmont transition zone, ecological restoration areas, and suburban expansion fringes exhibit higher response sensitivity. Consequently, land use management should move beyond mere quantity control. Greater attention should be paid to the location of land conversion, landscape connectivity, and the ecological functions of distinct land-use categories. Optimizing spatial allocation can help enhance the overall ecological benefits of land use.

5.4. Ecosystem Service Response Strategies for Territorial Spatial Zoning Control

The spatial heterogeneity of ESV in Xi'an reflects the combined effects of ecological conservation in the Qinling Mountains, cropland preservation on the Guanzhong Plain, and construction land expansion. The southern Qinling Mountains serve as the primary area supporting the city's ESV and should be regarded as the key zone for maintaining the ecological conservation control boundary and the Qinling ecological-security configuration. This northern piedmont zone of the Qinling Mountains exhibits strong potential for improving ecosystem services, but it is also a sensitive transition area where ecological space, agricultural land, and urban construction land intersect. In the central and northern Guanzhong Plain, cropland protection and urban expansion generate persistent spatial competition. The protection of permanent basic farmland faces particular challenges from construction land growth in this region. The central urban area and high-density built-up districts present a different set of issues, characterized by low ESV and concentrated negative responses. Accordingly, Xi'an's territorial spatial governance should adopt zoning-based strategies that integrate ecosystem service enhancement with construction land control and cropland preservation.

(1) Strengthening the protection of the southern Qinling ecological barrier to maintain the core source of ecosystem services in Xi'an.

The northern piedmont belt of the Qinling Mountains constitutes a critical interface for enhancing ESV in Xi'an. The assessment of improvement potential shows that the high-priority areas are mainly distributed in Lantian County, southeastern Chang'an District, southeastern Baqiao District, and southern Lintong District. These areas form a transitional belt connecting the Qinling ecological space, the agricultural landscapes of the Guanzhong Plain, and the urban fringe of Xi'an. Owing to the coexistence of forest land, grassland, water bodies, and cultivated land, this region provides a favorable ecological basis for improving ecosystem service functions. However, its location at the mountain–plain–urban interface also makes it sensitive to multiple land-use pressures, including construction land expansion, transportation infrastructure development, rural settlement growth, and cropland restructuring. Therefore, the piedmont transition zone should be regarded as a priority area where opportunities for ESV enhancement coexist with potential risks of ecological disturbance.

In terms of governance, the ecological protection red line and Qinling ecological protection requirements should be treated as strict spatial constraints. The expansion of construction land, tourism facilities, and transportation corridors into mountain ecological spaces should be carefully restricted to avoid the fragmentation of continuous forest land,

water conservation areas, and mountain ecological corridors. For fragmented forest patches, exposed slopes, and soil erosion-prone areas, near-natural restoration approaches should be adopted. Measures such as enclosure-based protection, supplementary planting of native tree species, slope vegetation restoration, and integrated small-watershed management can be used to improve water conservation, soil retention, and biodiversity maintenance functions. Low-intensity ecological recreation, nature education, and ecological science popularization may be introduced in appropriate areas, but they should not be developed as substitutes for ecological protection. High-intensity scenic-area construction and commercial tourism development should be prevented from weakening the ecosystem service functions of the Qinling Mountains.

(2) Identifying ecological improvement areas in the piedmont transition zone to promote ecological restoration and ecosystem service enhancement.

The piedmont transition zone along the northern Qinling Mountains is a key area for improving ESV in Xi'an. The improvement-potential results show that these areas are mainly located in Lantian County, southeastern Chang'an District, southeastern Baqiao District, and southern Lintong District. Spatially, they lie at the interface among the Qinling ecological space, the Guanzhong Plain agricultural space, and the urban construction space, making them important transition zones in Xi'an's ecological security pattern. This region has a relatively favorable ecological foundation, including forest land, grassland, and water systems. However, it is also affected by urban expansion, transportation construction, village and town development, and cropland-use adjustment. As a result, the piedmont transition zone has both strong potential for ecosystem service enhancement and a high risk of development disturbance.

Governance in this area should move beyond simple boundary control and adopt an integrated approach based on restoration–connectivity–enhancement. First, priority should be given to restoring fragmented forest land, inefficient construction edges, exposed slope patches, and degraded farmland. Measures such as native vegetation restoration, ecological buffer construction, and small-scale ecological patch supplementation can improve water conservation, soil retention, and biodiversity maintenance in the piedmont zone. Second, river corridors such as the Chan River, Ba River, and Feng River, together with the piedmont greenbelt, should be used to build a blue–green network connecting Qinling ecological space with peripheral urban green spaces. This can reduce ecological fragmentation and improve connectivity between the Qinling ecological barrier and the urban fringe. For areas with high improvement potential but strong development pressure, construction expansion should be strictly guided away from key ecological corridors and ecological restoration nodes to prevent further fragmentation of the piedmont ecological transition space.

(3) Strengthening the regulation of agricultural–urban interface areas in the Guanzhong Plain to coordinate cropland protection and urban development.

Land-use conversion analysis indicates that between 2000 and 2020, construction land expansion in Xi'an was primarily concentrated along the central urban fringe and the central–northern plain. The transformation of cultivated land into construction land constituted the dominant prevailing conversion. Lintong and Gaoling districts, Yanliang District, northern Chang'an District, and northern Huyi District lie within the interface zone between the agricultural space of the Guanzhong Plain and the outward expansion area of the metropolitan region. These areas are major cropland distribution zones but also face future demands for industrial development, transportation infrastructure, and urban growth. Consequently, the central challenge in this region is not solely ecological protection but rather the spatial competition between food production space and metropolitan development needs.

For these agricultural–urban interface areas, governance should prioritize cropland preservation, construction boundary control, and efficient use of existing construction land. Permanent basic farmland and high-quality cropland must be strictly protected, and their conversion to construction land should be restricted. Particular attention should be paid to preventing disorderly urban sprawl along transportation corridors, industrial parks, and suburban fringe areas. Concurrently, newly designated construction land should be utilized more efficiently. Priority should be given to the renewal of existing construction land, the redevelopment of inefficient industrial land, and the consolidation of village and township construction land to reduce incremental occupation of peripheral cropland. Ecological buffer zones, irrigation canal green corridors, and rural ecological corridors can be arranged along urban expansion fringes to mitigate the disturbance of construction activities to agricultural space and ecosystem services. Overall, governance in the agricultural–urban fringe areas of the Guanzhong Plain should integrate permanent basic farmland protection, urban growth boundary control, stock land renewal, and cropland quality improvement, thereby harmonizing urban development with agricultural space protection.

(4) Strengthening the ecological compensation capacity of the ancient city and high-density built-up areas to address shortcomings in urban ecosystem services.

Specifically, priority should be given to pocket parks, street greening, rooftop greening, vertical greening, rain gardens, permeable pavements, and small-scale water retention spaces. Existing parks, school open spaces, community green spaces, and riverfront public spaces can be connected through green corridors and slow-traffic networks to enhance ecological connectivity. In old urban districts where land resources are limited, ecological compensation should focus on micro-renewal and multifunctional use of public space to improve climate regulation, stormwater retention, recreational services, and residents' access to green space.

Specifically, ecological compensation in the central urban area and high-density built-up districts should rely on the refined renewal of existing urban spaces. Small ecological spaces, including pocket parks, street-corner greenery, community micro-green spaces, street trees, rooftop greening, and vertical greening, can be embedded into urban renewal projects to improve climate regulation, environmental purification, and recreational functions in dense built-up environments. For the historic urban area, large-scale demolition-oriented greening should be avoided. Instead, ecological compensation should be adapted to the existing urban fabric through courtyard greening, street and alley greening, the improvement of open spaces around the city wall, and the connection of slow-traffic green corridors. In combination with sponge city construction, rain gardens, sunken green spaces, permeable pavements, and ecological drainage systems can be improved to enhance internal hydrological regulation. In areas where continuous green space is insufficient, existing parks, rivers, community green spaces, campus green spaces, and urban open spaces can be connected through blue–green corridors to gradually form a more continuous urban ecological network. The priority should be to compensate for the weak ecosystem service capacity of construction land through refined stock-space renewal, thereby improving the ecological resilience of the central urban area and residents' environmental well-being.

5.5. Research Limitations and Future Directions

By linking MOP, PLUS, ESV assessment, SI, and LRI, this study examined scenario-based land use adjustment, ESV response, and spatial differentiation in Xi'an. Nevertheless, several sources of uncertainty should be noted.

First, uncertainty may arise from the consistency of multi-source datasets. The input data, including land use, natural environmental variables, socioeconomic data, location–transportation factors, and planning/statistical materials, were collected from different

sources. These datasets differ in spatial resolution, temporal coverage, and statistical standards. Although projection transformation, resampling, standardization, and classification integration were applied to improve comparability, scale mismatches among datasets may still affect the PLUS simulation and ESV assessment results. Future studies could introduce higher-resolution remote sensing imagery, refined territorial survey data, and detailed urban blue–green space datasets. Such data would make it possible to identify ecological spaces embedded within construction land more accurately and to capture small-scale land use changes that are difficult to distinguish under the current six-category classification system.

Second, the temporal configuration of the simulation also entails certain limitations. The present study adopted 2020 as the benchmark year and projected land-use configurations and ESV responses to 2040, establishing a 20-year medium- to long-term observation window. However, the main modeling process did not incorporate land use data from the 2020–2025 period. Consequently, recent changes related to construction land expansion, ecological restoration, and territorial spatial regulation in Xi'an may not have been fully accounted for. Future research could employ 2025 land use data as an updated baseline or as an independent validation dataset, provided that data source consistency, classification comparability, and temporal alignment with socioeconomic data can be ensured. Additionally, scenario time points such as 2030, 2035, and 2060 could be introduced to align with the Sustainable Development Goals, territorial spatial planning periods, and the long-term carbon neutrality target. This would help reveal the dynamic evolution of land use change alongside ESV responses over varying temporal horizons.

Regarding model constraints, the current framework still exhibits limitations in representing policy boundaries and external disturbances. The PLUS model identifies spatial land use conversion primarily through natural environmental variables, socioeconomic factors, and location-transportation accessibility. In contrast, constraints such as total ecological land area, permanent basic farmland, and construction land scale were introduced mainly through the MOP model at the quantity-structure level. Consequently, policy-based spatial boundaries—including ecological protection red lines, urban growth boundaries, Qinling protection zones, and water source protection areas—were not fully embedded into the PLUS-based spatial allocation process. External disturbance factors also remain insufficiently accounted for. Sudden events such as extreme rainfall, floods, droughts, and landslides are highly uncertain and were not explicitly included as independent variables in the 2040 scenario simulation. Future research could incorporate the "three control lines" of territorial spatial planning, disaster risk zoning, climate change scenarios, and ecological vulnerability assessment to construct more refined policy constraint layers and disturbance scenarios. In addition, although the random forest algorithm within the PLUS framework was employed to infer land-use expansion likelihoods, the importance rankings of driving factors were not retained for separate comparison. Therefore, the choice of driving determinants was justified primarily according to land use change mechanisms, regional geographical characteristics, and data availability. Future studies should further output and compare the importance associated with driving determinants for each land use type to enhance model interpretability.

This ESV assessment also involves methodological simplifications. The equivalence-factor approach is well-suited to regional-scale comparisons, but its reliance on aggregated land use categories limits its ability to capture fine ecological differences. For example, it cannot fully distinguish vertical zonation within Qinling mountain forests, differences between natural and planted forests, or functional variations among wetland types in the Weihe River Basin. Therefore, the ESV results should be interpreted primarily as a basis for scenario comparison and spatial pattern identification, rather than as precise monetary

estimates of each ecosystem service. Assigning a zero ESV coefficient to construction land at the first-level land use classification helps avoid overestimating the ecological value of artificial built-up areas. However, this treatment may underestimate ecosystem service contributions from ecological spaces embedded within construction land, such as urban green spaces, parks, urban water bodies, constructed wetlands, and sponge facilities. Future research could introduce more detailed datasets on urban green space, blue-green networks, wetland boundaries, and impervious surfaces. Process-based models—such as InVEST Carbon Storage, Habitat Quality, CASA, and RUSLE—could also be integrated to more accurately assess key ecosystem-service functions, including carbon-retention capacity, habitat suitability, hydrological regulation, as well as soil-retention functions.

The SI and LRI indicators also introduce methodological uncertainty. Although they help distinguish regional ESV sensitivity from local response heterogeneity, the LRI results may be influenced by the selected standardization method and the thresholds used to classify response levels. Future work should examine how LRI outputs change under different spatial units and classification schemes. Field surveys, expert judgment, and ecological monitoring records could also be used to verify whether the high-response areas identified by LRI correspond to actual ecological improvement or degradation, thereby strengthening the reliability of the response analysis.

The conclusions are also shaped by the specific territorial context of Xi'an. The city is characterized by the spatial overlap of the Qinling Ecological Barrier, the agricultural space of the Guanzhong Plain, and the outward expansion of the central urban area. Therefore, the spatial differentiation patterns and zoning governance strategies identified in this study have a certain degree of local specificity. To test the broader applicability of the MOP–PLUS–ESV–SI/LRI framework, future comparative studies could include coastal cities, resource-based cities, mountainous cities, and core cities within urban agglomerations. Such comparisons would help assess how well the framework can be transferred to different territorial contexts.

6. Conclusions

This study examined how alternative land use pathways may affect ecosystem service value in Xi'an. By combining land demand estimation, spatial allocation simulation, ESV assessment, and response index analysis, the study identified historical land use transitions, projected 2040 land use patterns, and evaluated regional and local ESV responses. The main findings are summarized as follows:

(1) During the period from 2000 to 2020, Xi'an's land use pattern maintained a clear spatial division: a southern ecological mountain zone and a central-northern agricultural-urban zone. Forest land was predominantly aggregated within the Qinling Mountains, cropland occupied the plains as well as tablelands, and construction land continued to expand outward from the urban core. Most newly expanded construction land originated from cropland conversion, reflecting the pressure of urbanization on suburban agricultural space. Meanwhile, the southern Qinling forest area remained relatively stable and continued to serve as the principal spatial foundation underpinning regional ESV.

(2) Scenario simulations for 2040 indicate that the ecological outcomes of land use adjustment depend strongly on the chosen development pathway. The economic priority scenario generated the most substantial expansion of construction land while producing the lowest total ESV. Conversely, the ecological-conservation pathway increased forest land extent and yielded the highest total ESV. Both the baseline-evolution and integrated-coordination pathways showed moderate ESV declines relative to the 2020 baseline. Overall, forest land remained the dominant contributor to regional ESV,

while construction land growth, together with shifts in forest land area, constituted the key drivers of differences among scenarios.

(3) The response index results indicate that ESV changes in Xi'an exhibit both regional sensitivity and local spatial differentiation. At the regional level, the ecological protection scenario was associated with a positive ESV response, whereas the economic priority scenario triggered the strongest negative response. At the local level, positive responses appeared mainly in areas where ecological land improved, including the northern Qinling piedmont zone, Lantian County, and southeastern Chang'an District. Negative responses were concentrated along the central urban fringe, the central-northern plain, and construction expansion zones. Zhouzhi County, Lantian County, Chang'an District, and Huyi District formed the main high-value ESV-supporting units, while the central urban districts remained low-value areas. These findings suggest that Xi'an's territorial spatial optimization should maintain the southern Qinling ecological barrier, restrict construction land expansion in the central-northern region, and enhance ecological restoration and blue-green connectivity in piedmont and suburban fringe areas.

Author Contributions: Conceptualization: Y.L., S.Z. and W.Z.; Methodology: Y.L., S.Z. and C.S.; Software: Y.L. and S.Z.; Validation: Y.L., S.Z. and C.S.; Formal Analysis: Y.L. and S.Z.; Investigation: Y.L., S.Z. and C.S.; Resources: W.Z. and S.Z.; Data Curation: Y.L. and S.Z.; Writing—Original Draft: Y.L.; Writing—Review and Editing: Y.L., S.Z., W.Z. and C.S.; Visualization: Y.L. and S.Z.; Supervision: W.Z.; Project Administration: W.Z.; Funding Acquisition: W.Z. All authors have read and agreed to the published version of the manuscript.

Funding: This research was funded by the 2026 "Double First-Class" Construction Funded Project of Xi'an Academy of Fine Arts, grant number XK202601. The project title is "Artistic Exchange and Cultural Integration along the Silk Road: Environmental System Regeneration and Dissemination of Local Heritage Remains".

Institutional Review Board Statement: Not applicable.

Informed Consent Statement: Not applicable.

Data Availability Statement: Data will be made available on request.

Acknowledgments: We gratefully acknowledge the financial support that made this research possible. We also sincerely thank the local government and residents for their assistance and cooperation during the field investigation and data collection process.

Conflicts of Interest: The authors declare no conflicts of interest.

References

1. Foley, J.A.; DeFries, R.; Asner, G.P.; Barford, C.; Bonan, G.; Carpenter, S.R.; Chapin, F.S.; Coe, M.T.; Daily, G.C.; Gibbs, H.K.; et al. Global consequences of land use. *Science* **2005**, *309*, 570–574. [CrossRef] [PubMed]
2. Shin, Y.J.; Arneth, A.; Chowdhury, R.R.; Midgley, G.F.; Alkemade, J.R.M. Plausible futures of nature, its contributions to people and their good quality of life. In *The Global Assessment Report on Biodiversity and Ecosystem Services*; Intergovernmental Science-Policy Platform on Biodiversity and Ecosystem: Bonn, Germany, 2019; pp. 599–766.
3. Costanza, R.; De Groot, R.; Braat, L.; Kubiszewski, I.; Fioramonti, L.; Sutton, P.; Farber, S.; Grasso, M. Twenty years of ecosystem services: How far have we come and how far do we still need to go? *Ecosyst. Serv.* **2017**, *28*, 1–16. [CrossRef]
4. Peng, Q.; Dilinuer, A.; Li, P.; Hu, C.; Kang, J. Spatial and temporal evolution and driving factors of ecosystem service value in the Kaidu River basin. *J. Agric. Resour. Environ.* **2025**, *42*, 911.
5. Zhang, P.; Liu, L.; Yang, L.; Zhao, J.; Li, Y.; Qi, Y.; Cao, L. Exploring the response of ecosystem service value to land use changes under multiple scenarios coupling a mixed-cell cellular automata model and system dynamics model in Xi'an, China. *Ecol. Indic.* **2023**, *147*, 110009.
6. Wu, C.; Wang, Z. Multi-scenario simulation and evaluation of the impacts of land use change on ecosystem service values in the Chishui River Basin of Guizhou Province, China. *Ecol. Indic.* **2024**, *163*, 112078. [CrossRef]

7. Liu, J.; Zhang, L.; Zhang, N. Analyzing the South-North gap in the high-quality development of China's urbanization. *Sustainability* **2022**, *14*, 2178.
8. Sheng, S.; Yang, B.; Kuang, B. Impact of cereal production displacement from urban expansion on ecosystem service values in China: Based on three cropland supplement strategies. *Int. J. Environ. Res. Public Health* **2022**, *19*, 4563. [CrossRef] [PubMed]
9. Ma, X.; Li, J.; Li, G. Simulation and multi-scenario prediction of land-use change in the Gansu section of the Yellow River Basin, China. *Front. Environ. Sci.* **2024**, *12*, 1403248.
10. Verburg, P.H.; Soepboer, W.; Veldkamp, A.; Limpiada, R.; Espaldon, V.; Mastura, S.S.A. Modeling the spatial dynamics of regional land use: The CLUE-S model. *Environ. Manag.* **2002**, *30*, 391–405. [CrossRef]
11. Tang, H.; Halike, A.; Yao, K.; Wei, Q.; Yao, L.; Tuheti, B.; Luo, J.; Duan, Y. Ecosystem service valuation and multi-scenario simulation in the Ebinur Lake Basin using a coupled GMOP-PLUS model. *Sci. Rep.* **2024**, *14*, 5071. [PubMed]
12. Chen, G.; Zhang, D.; Zhao, J.; Zhang, L. Land use and climate change-based multi-scenario simulation of ecosystem service trade-offs/synergies: A case study of the central Yunnan urban agglomeration, China. *PLoS ONE* **2025**, *20*, e0324015. [PubMed]
13. Gong, J.; Du, H.; Sun, Y.; Zhan, Y. Simulation and prediction of land use in urban agglomerations based on the PLUS model: A case study of the Pearl River Delta, China. *Front. Environ. Sci.* **2023**, *11*, 1306187. [CrossRef]
14. Pontius, G.R.; Malanson, J. Comparison of the structure and accuracy of two land change models. *Int. J. Geogr. Inf. Sci.* **2005**, *19*, 243–265. [CrossRef]
15. Tang, L.; Li, J.; Xie, C.; Wang, M. Multi-Scenario Simulation of Ecosystem Service Value in Xiangjiang River Basin, China, Based on the PLUS Model. *Land* **2025**, *14*, 1482. [CrossRef]
16. Zhang, M.; Chen, E.; Zhang, C.; Liu, C.; Li, J. Multi-scenario simulation of land use change and ecosystem service value based on the markov–FLUS model in Ezhou city, China. *Sustainability* **2024**, *16*, 6237.
17. Jiang, Y.; Du, G.; Teng, H.; Wang, J.; Li, H. Multi-scenario land use change simulation and spatial response of ecosystem service value in black soil region of northeast China. *Land* **2023**, *12*, 962. [CrossRef]
18. Shu, R.; Wang, Z.; Guo, N.; Wei, M.; Zou, Y.; Hou, K. Multi-scenario land use optimization simulation and ecosystem service value estimation based on fine-scale land survey data. *Land* **2024**, *13*, 557.
19. Fu, X.; Wang, X.; Yang, Y.J. Deriving suitability factors for CA-Markov land use simulation model based on local historical data. *J. Environ. Manag.* **2018**, *206*, 10–19. [CrossRef]
20. Wang, S.-D.; Wang, X.-C.; Zhang, H.-B. Simulation on optimized allocation of land resource based on DE-CA model. *Ecol. Model.* **2015**, *314*, 135–144. [CrossRef]
21. Cao, S.; Jin, X.-B.; Yang, X.-H.; Sun, R.; Liu, J.; Han, B.; Xu, W.-Y.; Zhou, Y.-K. Coupled MOP and GeoSOS-FLUS models research on optimization of land use structure and layout in Jintan district. *J. Nat. Resour.* **2019**, *34*, 1171–1185.
22. Shi, Q.; Gu, C.-J.; Xiao, C. Multiple scenarios analysis on land use simulation by coupling socioeconomic and ecological sustainability in Shanghai, China. *Sustain. Cities Soc.* **2023**, *95*, 104578. [CrossRef]
23. Zhang, X.; Ren, W.; Peng, H. Construction landuse change simulation and spatial responses of ecosystem service value under multiple scenarios: A case study of Wuhan, China. *Ecol. Indic.* **2022**, *144*, 109526.
24. Bai, J.; Jia, Z.; Sun, Y.; Zheng, C.; Wen, M. Multi-Scenario Simulation of Land Use Change Along with Ecosystem Service Value for the Lanzhou–Xining Urban Agglomeration. *Land* **2025**, *14*, 860.
25. Peng, K.; Jiang, W.; Ling, Z.; Hou, P.; Deng, Y. Evaluating the potential impacts of land use changes on ecosystem service value under multiple scenarios in support of SDG reporting: A case study of the Wuhan urban agglomeration. *J. Clean. Prod.* **2021**, *307*, 127321. [CrossRef]
26. Guo, P.; Zhang, F.; Wang, H. The response of ecosystem service value to land use change in the middle and lower Yellow River: A case study of the Henan section. *Ecol. Indic.* **2022**, *140*, 109019. [CrossRef]
27. Xiao, Y.; Huang, M.; Xie, G.; Zhen, L. Evaluating the impacts of land use change on ecosystem service values under multiple scenarios in the Hunshandake region of China. *Sci. Total Environ.* **2022**, *850*, 158067. [CrossRef] [PubMed]
28. Sujetovienė, G.; Dabašinskas, G. Ecosystem service value changes in response to land use dynamics in Lithuania. *Land* **2023**, *12*, 2151. [CrossRef]
29. Kreuter, U.P.; Harris, H.G.; Matlock, M.D.; E Lacey, R. Change in ecosystem service values in the San Antonio area, Texas. *Ecol. Econ.* **2001**, *39*, 333–346. [CrossRef]
30. Li, T.H.; Li, W.K.; Qian, Z.H. Variations in ecosystem service value in response to land use changes in Shenzhen. *Ecol. Econ.* **2010**, *69*, 1427–1435. [CrossRef]
31. Aschonitis, V.; Gaglio, M.; Castaldelli, G.; Fano, E.A. Criticism on elasticity-sensitivity coefficient for assessing the robustness and sensitivity of ecosystem services values. *Ecosyst. Serv.* **2016**, *20*, 66–68. [CrossRef]
32. Shao, Y.; Yuan, X.; Ma, C.; Ma, R.; Ren, Z. Quantifying the spatial association between land use change and ecosystem services value: A case study in Xi'an, China. *Sustainability* **2020**, *12*, 4449. [CrossRef]
33. Zhao, Y.; Han, Z.; Yan, X.; Wang, X. Integrating spatial heterogeneity into an analysis between ecosystem service value and its driving factors: A case study of Dalian, China. *Int. J. Environ. Res. Public Health* **2022**, *19*, 17055. [CrossRef] [PubMed]

34. Han, L.; Li, Y.; Ge, Z.; Fang, F.; Gao, L.; Zhang, J.; Du, Z.; Cui, L. Study on the spatial and temporal evolution of ecosystem service value based on land use change in Xi'an City. *Sci. Rep.* **2025**, *15*, 66. [CrossRef] [PubMed]
35. Peng, L.; Zhang, L.; Li, X.; Wang, Z.; Wang, H.; Jiao, L. Spatial expansion effects on urban ecosystem services supply-demand mismatching in Guanzhong Plain Urban Agglomeration of China. *J. Geogr. Sci.* **2022**, *32*, 806–828. [CrossRef]
36. Wang, Y.; Li, X.; Zhang, Q.; Li, J.; Zhou, X. Projections of future land use changes: Multiple scenarios-based impacts analysis on ecosystem services for Wuhan city, China. *Ecol. Indic.* **2018**, *94*, 430–445. [CrossRef]
37. Zhu, L.; Huang, Y. Multi-scenario simulation of ecosystem service value in Wuhan metropolitan area based on PLUS-GMOP model. *Sustainability* **2022**, *14*, 13604.
38. Lou, Y.; Yang, D.; Zhang, P.; Zhang, Y.; Song, M.; Huang, Y.; Jing, W. Multi-scenario simulation of land use changes with ecosystem service value in the Yellow River Basin. *Land* **2022**, *11*, 992. [CrossRef]
39. Xie, G.D.; Zhang, C.X.; Zhang, L.M.; Chen, W.H.; Li, S.M. Improvement of the evaluation method for ecosystem service value based on per unit area. *J. Nat. Resour.* **2015**, *30*, 1243–1254.
40. Sannigrahi, S.; Bhatt, S.; Rahmat, S.; Paul, S.K.; Sen, S. Estimating global ecosystem service values and its response to land surface dynamics during 1995–2015. *J. Environ. Manag.* **2018**, *223*, 115–131. [CrossRef]
41. Sharma, S.; Hussain, S.; Singh, A.N. Impact of land use and land cover on urban ecosystem service value in Chandigarh, India: A GIS-based analysis. *J. Urban Ecol.* **2023**, *9*, juac030. [CrossRef]
42. Yu, H.; Yang, J.; Sun, D.; Li, T.; Liu, Y. Spatial responses of ecosystem service value during the development of urban agglomerations. *Land* **2022**, *11*, 165. [CrossRef]
43. Chen, J.; Sun, B.-M.; Chen, D.; Wu, X.; Guo, L.-Z.; Wang, G. Land use changes and their effects on the value of ecosystem services in the small Sanjiang plain in China. *Sci. World J.* **2014**, *2014*, 752846. [CrossRef]
44. Arsanjani, J.J.; Tayyebi, A.; Vaz, E. GlobeLand30 as an alternative fine-scale global land cover map: Challenges, possibilities, and implications for developing countries. *Habitat Int.* **2016**, *55*, 25–31.
45. Huang, Y.H.; Jiang, D.; Fu, J.Y. China Kilometer-Grid GDP Distribution Dataset. *J. Geogr. Sci.* **2014**, *69*, 45–48.
46. Fu, J.; Jiang, D.; Huang, Y. *KM Grid Population Dataset of China (PopulationGrid_China)*; Global Change Research Data Publishing & Repository: Beijing, China, 2014.
47. Elvidge, C.D.; Zhizhin, M.; Ghosh, T.; Hsu, F.-C.; Taneja, J. Annual time series of global VIIRS nighttime lights derived from monthly averages: 2012 to 2019. *Remote Sens.* **2021**, *13*, 922. [CrossRef]
48. Xin, S.; Li, Z.; Chen, N.; Zhang, Z.; Zhang, X.; Chen, H.; Ma, X.; Kang, L. The contribution of multi-objective land use optimization to reducing ecological risk: A case study of the Lanzhou-Xining urban agglomeration. *Ecol. Indic.* **2024**, *168*, 112604.
49. Lee, J.; Yin, X.; Zhu, H. Spatial optimization of land use allocation based on the trade-off of carbon mitigation and economic benefits: A study in Tianshan north slope urban agglomeration. *Land* **2024**, *13*, 892. [CrossRef]
50. Costanza, R.; d'Arge, R.; de Groot, R.; Farber, S.; Grasso, M.; Hannon, B.; Limburg, K.; Naeem, S.; O'Neill, R.V.; Paruelo, J.; et al. The value of the world's ecosystem services and natural capital. *Nature* **1997**, *387*, 253–260. [CrossRef]
51. Liu, X.; Liang, X.; Li, X.; Xu, X.; Ou, J.; Chen, Y.; Li, S.; Wang, S.; Pei, F. A future land use simulation model (FLUS) for simulating multiple land use scenarios by coupling human and natural effects. *Landsc. Urban Plan.* **2017**, *168*, 94–116. [CrossRef]
52. Li, S.; Bing, Z.; Jin, G. Spatially explicit mapping of soil conservation service in monetary units due to land use/cover change for the Three Gorges Reservoir Area, China. *Remote Sens.* **2019**, *11*, 468. [CrossRef]
53. Chen, S.; Liu, X.; Yang, L.; Zhu, Z. Variations in ecosystem service value and its driving factors in the Nanjing metropolitan area of China. *Forests* **2023**, *14*, 113. [CrossRef]

Disclaimer/Publisher's Note: The statements, opinions and data contained in all publications are solely those of the individual author(s) and contributor(s) and not of MDPI and/or the editor(s). MDPI and/or the editor(s) disclaim responsibility for any injury to people or property resulting from any ideas, methods, instructions or products referred to in the content.